Published in final edited form as:
Biochemistry. 2007 September 4; 46(35): 10170–10185. doi:10.1021/bi700017z.

THE GROUP VIA CALCIUM-INDEPENDENT PHOSPHOLIPASE A_2 ($iPLA_2\beta$) PARTICIPATES IN ER STRESS-INDUCED INS-1 INSULINOMA CELL APOPTOSIS BY PROMOTING CERAMIDE GENERATION VIA HYDROLYSIS OF SPHINGOMYELINS BY NEUTRAL SPHINGOMYELINASE[†,1]

Xiao-Yong Lei, **Sheng Zhang**, **Alan Bohrer**, **Shunzhong Bao**, **Haowei Song**, and **Sasanka Ramanadham**[*]
Department of Medicine, Mass Spectrometry Resource and Division of Endocrinology, Metabolism, and Lipid Research, Washington University School of Medicine, St. Louis, MO 63110

Abstract

β-cell mass is regulated by a balance between β-cell growth and β-cell death, due to apoptosis. We previously reported that apoptosis of INS-1 insulinoma cells due to thapsigargin-induced ER stress was suppressed by inhibition of the Group VIA Ca^{2+}-independent phospholipase A_2 ($iPLA_2\beta$), associated with increased ceramide generation, and that the effects of ER stress were amplified in INS-1 cells in which $iPLA_2\beta$ was over expressed (OE INS-1 cells). These findings suggested that $iPLA_2\beta$ and ceramides participate in ER stress-induced INS-1 cell apoptosis. Here, we addressed this possibility and also the source of the ceramides by examining the effects of ER stress in empty vector (V)-transfected and $iPLA_2\beta$-OE INS-1 cells using apoptosis assays and immunoblotting, quantitative PCR, and mass spectrometry analyses. ER stress induced expression of ER stress factors GRP78 and BiP, cleavage of apoptotic factor PARP, and apoptosis in V and OE INS-1 cells. Ceramide accumulation during ER stress was not associated with changes in mRNA levels of serine palmitoyl-transferase (SPT), the rate-limiting enzyme in *de novo* synthesis of ceramides but both message and protein levels of neutral sphingomyelinase (NSMase), which hydrolyzes sphingomyelins to generate ceramides, temporally increased in the INS-1 cells. The increases in NSMase expression in the ER-stressed INS-1 cells were associated with corresponding temporal elevations in ER-associated $iPLA_2\beta$ protein and catalytic activity. Pretreatment with BEL inactivated $iPLA_2\beta$ and prevented induction of NSMase message and protein in ER-stressed INS-1 cells. Relative to V INS-1 cells, the effects of ER stress were accelerated and/or amplified in the OE INS-1 cells. However, inhibition of $iPLA_2\beta$ or NSMase (chemically or with siRNA) suppressed induction of NSMase message, ceramide generation, sphingomyelin hydrolysis, and apoptosis in both V and OE INS-1 cells during ER stress. In contrast, inhibition of SPT did not suppress ceramide generation or apoptosis in either V or OE INS-1 cells. These findings indicate that $iPLA_2\beta$ activation participates in ER stress-induced INS-1 cell apoptosis by promoting ceramide generation via NSMase-catalyzed hydrolysis of

[†]This work was supported by grants from the National Institutes of Health (RO1-69455, R37-DK34388, P01-HL57278, P41-RR00954, P60-DK20579, and P30-DK56341).

[1]The abbreviations used are: BEL, bromoenol lactone suicide inhibitor of $iPLA_2\beta$; $cPLA_2$, group IV cytosolic phospholipase A_2; ER, endoplasmic reticulum; ESI, electrospray ionization; GPC, glycero-phosphocholine; $iPLA_2\beta$, β-isoform of group VIA calcium-independent phospholipase A_2; MitoMP, mitochondrial membrane potential, MS, mass spectrometry; NSMase, neutral sphingomyelinase; OE, $iPLA_2\beta$-overexpressing cells; PLA_2, phospholipase A_2; SEM, standard error of the mean; SERCA, sarcoendoplasmic reticulum Ca^{2+}-ATPase; SPT, serine palmitoyl transferase.

*Address correspondence to: Sasanka Ramanadham, Dept. Medicine, Washington University School of Medicine, Campus Box 8127, 660 S. Euclid Ave., St. Louis, MO 63110; telephone 314-362-8194; FAX 314-362-7641; E-mail: sramanad@im.wustl.edu.

sphingomyelins, raising the possibility that this pathway contributes to β-cell apoptosis due to ER stress.

Diabetes mellitus is the most prevalent human metabolic disease, and it results from loss and/or dysfunction of β-cells in pancreatic islets. Type 1 diabetes mellitus is caused by autoimmune β-cell destruction (1) and apoptosis plays a prominent role in the loss of β-cells during development of Type 1 diabetes mellitus (1,2). Type 2 diabetes mellitus results from a progressive decline of β-cell function and chronic insulin resistance which is characterized by initial peripheral insulin resistance and compensatory hyperinsulinemia that is followed by loss in β-cell function and frank hyperglycemia (3–6).

Autopsy studies indicate that the β-cell mass in obese Type 2 diabetes mellitus patients is smaller than that in obese non-diabetic subjects (7–9) and recent studies demonstrated that the loss in β-cell function in non-obese Type 2 diabetes mellitus is also associated with decreases in β-cell mass (10,11). β-cell mass is regulated by a balance between β-cell growth, resulting from β-cell replication and neogenesis, and β-cell death resulting from apoptosis (12,13). Findings in both rodent models of Type 2 diabetes mellitus (14–16) and in human T2 diabetes mellitus (10,11) have now led to the conclusion that the decrease in β-cell mass in Type 2 diabetes mellitus is not attributable to reduced β-cell proliferation or neogenesis but to increased β-cell apoptosis. This conclusion is also supported by observations from other studies (17–20). It is therefore important to understand the mechanisms underlying β-cell apoptosis if this process is to be prevented or delayed.

Agents that induce β-cell apoptosis (21) act via an extrinsic pathway involving interaction with death receptors residing in the plasma membrane or via an intrinsic pathway involving mitochondrial signaling (22,23). A third organelle gaining prominence as a participant in apoptosis is the endoplasmic reticulum (ER) (22–26). In addition to serving as a cellular Ca^{2+} store, ER is the site where secretory proteins are synthesized, assembled, folded, and post-translationally modified. Interruption of any of these functions can lead to production of malfolded proteins that require rapid degradation of mutant proteins. An imbalance between the load of client proteins on the ER and the ER's ability to process the load results in ER stress (27,28). Prolonged ER stress promotes induction of stress factors and activation of caspase-12, localized in ER (23,25,26,29), and can subsequently lead to apoptotic cell death. Downstream, all three pathways activate caspase-3, a protease that is central to execution of apoptosis (30). Being a site for Ca^{2+} storage, the ER responds to various stimuli to release Ca^{2+} and is therefore extremely sensitive to changes in cellular homeostasis. A number of factors can induce ER stress and this process is thought to be a cause of various diseases, including Alzheimer's and Parkinson's diseases (31).

Secretory function of β-cells endows them with a highly developed ER and heightens their susceptibility to ER stress. Mutations in genes encoding the ER-stress transducer pancreatic ER kinase (PERK) (32) and the ER resident protein involved in degradation of malfolded ER proteins are linked to diminished β-cell health clinically (33,34). Further, in the Akita diabetic mouse, mutation in the *Ins2*^{C96Y} gene produces an abnormal insulin product that accumulates in the ER. This leads to increased expression of the ER chaperone protein GRP78 (BiP) and the ER stress marker CHOP (15,35–37) and a progressive decrease in β-cell mass, due to β-cell apoptosis, and subsequent hyperglycemia ensues.

The SERCA inhibitor thapsigargin (38) induces ER stress, promotes caspase-12 cleavage (22,25), and apoptosis of neurons and insulin releasing BRIN-BID11 cells (22) and Apaf-1 null cells (26). While SERCA inhibitors promote loss of ER Ca^{2+} stores, induction of MIN-6 cell apoptosis by these agents occurs by a pathway that does not require an increase in $[Ca^{2+}]_i$ but instead requires the generation of arachidonic acid metabolites (39). Thapsigargin-

induced ER stress in pancreatic islets leads to hydrolysis of arachidonic acid from membrane phospholipids also by a Ca^{2+}-independent mechanism that is suppressed by a bromoenol lactone (BEL) suicide-substrate inhibitor of Ca^{2+}-independent phospholipase A_2 ($iPLA_2\beta$) (40). These observations raised the possibility that $iPLA_2\beta$ participates in ER stress in β-cells.

The PLA_2s are a diverse group of enzymes that catalyze hydrolysis of the *sn*-2 substituent from glycerophospholipid substrates to yield a free fatty acid and a 2-lysophospholipid (41). At present, the recognized PLA_2s are classified into 15 groups based on their Ca^{2+} requirement for activation and sequence homology (42). Among the $iPLA_2$s is one that does not require Ca^{2+} for activity and is classified as a Group VIA $iPLA_2$ and is designated as the β-isoform of $iPLA_2$ ($iPLA_2\beta$) (43–45), distinguishing it from the membrane-associated γ-isoform ($iPLA_2\gamma$) (44). The $iPLA_2\beta$ enzyme is activated by ATP and is inhibited by BEL (46). While in macrophage-like cells $iPLA_2\beta$ is proposed to be involved in phospholipid remodeling (47), $iPLA_2\beta$ is thought to participate in signal transduction in other cells (48–53), including β-cells (43,46,54,55).

Recent findings in non-β-cells suggested another role for $iPLA_2\beta$. Induction of human U937 promonocyte apoptosis by anti-Fas antibody is associated with hydrolysis of arachidonic acid from membrane phospholipids by a mechanism that is inhibited by BEL and that is not catalyzed by $sPLA_2$ or $cPLA_2$ (56). U937 cell apoptosis is also associated with cleavage of $iPLA_2\beta$ by caspase-3, and overexpression of this $iPLA_2\beta$ cleavage product amplifies both thapsigargin-induced arachidonic acid release and cell-death (57). S49 lymphoma, PC12, and human coronary artery endothelial cell-death induced by thapsigargin (57,58), polychlorinated biphenyls (59), and polycyclic aromatic hydrocarbons (60), respectively, are all reported to be suppressed by inhibitors of PLA_2 including BEL. Collectively, these observations suggest that $iPLA_2\beta$, in part, contributes to events that promote apoptosis but the mechanism of its action has not yet been described.

Pancreatic islet β-cells and insulinoma cells express a $iPLA_2\beta$ activity that is sensitive to inhibition by BEL (46,54,61,62). We recently reported (63) that ER stress induces INS-1 insulinoma cell apoptosis and amplifies apoptosis of $iPLA_2\beta$-overexpressing (OE) INS-1cells and that this is inhibited by BEL. An intriguing finding associated with induction of ER stress in INS-1 cell apoptosis was an increase in ceramide generation that was also significantly amplified in OE INS-1 cells (63). Ceramides are lipid messengers that can suppress cell growth and induce apoptosis (64–66). In the present study, we examined the relationship between ER stress, ceramide generation, $iPLA_2\beta$, and INS-1 cell apoptosis.

Experimental Procedures

Materials

INS-1 insulinoma cells were provided by Dr. C. Newgard (Duke University Medical Center, Durham, NC). Other materials were obtained from the following (sources): (16:0/[^{14}C]-18:2)-GPC (PLPC, 55 mCi/mmol), rainbow molecular mass standards, and enhanced chemiluminescence reagent (Amersham, Arlington Heights, IL); SYBR Green PCR Kit (Applied Biosystems, Foster City, CA); brain and egg sphingomyelins, ceramide, and other lipid standards (Avanti Polar Lipids, Alabaster, AL); calnexin (BD Sciences, San Jose, CA); Coomassie reagent, SDS-PAGE supplies, and Triton X-100 (BioRad, Hercules, CA); mitochondrial membrane potential detection kit (Cell Tech. Inc., Mountain View, CA); retroviral vector siRNA reagents (Clontech, Mountain View, CA); paraformaldehyde (Electron Microscopy Sciences, Ft. Washington, PA); DNase-free RNase A (Gentra Systems Inc. Minneapolis, MN); RT-PCR reagents (Invitrogen, Carlsbad, CA); Immobilin-P PVDF membrane (Millipore Corp., Bedford, MA); complex IV antibody, Slow Fade® light antifade kit (Molecular Probes, Eugene, OR); RNeasy kit (Qiagen Inc., Valencia, CA); TUNEL kit

(Roche Diagnostic Corporation, Indianapolis, IN); all other primary and secondary antibodies (Santa Cruz Biotech. Inc., Santa Cruz, CA); and ER isolation kit, protease inhibitor cocktail, common reagents, and salts (Sigma Chemical Co., St. Louis, MO).

Preparation, culture, and treatment of stably-transfected INS-1 cells

A retroviral system (46,67) was used to stably transfect INS-1 cells with either empty retroviral vector (V INS-1 cells) or with a vector construct containing iPLA$_2$β cDNA (OE INS-1 cells), as described (43). The cells were cultured and passaged, as described (68), and grown to confluency in Petri dishes or flasks prior to treatment. The INS-1 cells were treated with either vehicle (DMSO, 0.50 μL/mL) alone or with thapsigargin (1 μM) to induce ER stress and incubated for up to 24 h. In some studies, the cells were co-incubated with an inhibitor of iPLA$_2$β (BEL, 10 μM), SPT (*l*-cycloserine, 1 μM), or NSMase (GW4869, 10 μM).

iPLA$_2$β activity assay in V and OE INS-1 cells

To verify that the INS-1 cells transfected with a construct containing iPLA$_2$β cDNA expressed higher iPLA$_2$β protein and catalytic activity, cytosol was prepared from these and V INS-1 cells, as described (63) and protein concentration was determined using Coomasie reagent. Immunoreactive-iPLA$_2$β protein was visualized, as described below, and iPLA$_2$β catalytic activity (in 25 μg protein aliquot) in the absence and presence of ATP (10 mM) or BEL (1 μM) was assayed and quantitated, as described (63).

To examine whether iPLA$_2$β expression in the ER is affected by ER stress, ER was prepared from vehicle- and thapsigargin-treated INS-1 cells, as described (69,70). Cells were harvested and washed twice (750g, 5 min, 4 °C) with 10 volumes of ice-cold phosphate-buffered saline. The cell pellet was suspended in 3 volumes of ice-cold isolation buffer (20 mM HEPES-KOH, pH 7.8, 250 mM sucrose, 1 mM EGTA, 10 mM potassium chloride, supplemented with protease inhibitor cocktail (50 μL/mL). The cells were placed on ice for 15 min and then transferred to a Dounce homogenizer (Kimble/Kontes, Vineland, NJ) and disrupted by douncing 50 times on ice. The homogenate was then centrifuged (15,000g, 15 min, 4 °C) and the supernatant was separated from the mitochondria-containing pellet and further centrifuged (100,000g, 1 h, 4 °C) to obtain an ER fraction. The pellet containing ER was then resuspended in HB buffer (40 mM Tris-HCl pH 7.8, 250 mM sucrose, 1 mM EGTA), sonicated, and protein concentration determined for iPLA$_2$β activity and immunoblotting assays. Enrichment of the fraction with ER was verified by immunoblotting analyses for various organelle markers: calnexin (ER), complex IV (mitochondria), FTCD 58K-9 (Golgi), Oct-1 (nuclei), and Na^+/K^+ ATPase (membrane).

Immunoblotting analyses

INS-1 cells were harvested at various times (0–24 h) following induction of ER stress, sonicated, and the homogenate centrifuged (100,000g, 1 h, 4 °C) to obtain cytosol. An aliquot (containing 30 μg protein) of homogenate, cytosol, ER, or mitochondria was analyzed by SDS-PAGE (8 or 15%), transferred onto Immobilin-P PVDF membranes, and processed for immunoblotting analyses, as described (63). The targeted proteins and the (1° antibody concentrations) were as follows: GRP78 (1:500), CHOP (1:500), PARP (1:1000), iPLA$_2$β (T-14; 1:500), calnexin (1:1,000), complex IV (1:2,000), FTCD 58K-9 (1:1,000), Oct-1 (1:1,000), and Na^+/K^+ ATPase (1:2000), NSMase (1:1,000) and tubulin control (1:2000). The secondary antibody concentration was 1:10,000. Immunoreactive bands were visualized by enhanced chemiluminescence.

Assays for apoptosis

To assess the incidence of apoptosis induced by ER stress TUNEL, DNA laddering, and mitochondrial membrane potential (MitoMP) analyses were performed as described below:

***In situ* detection of DNA cleavage by TUNEL staining—**At various times, INS-1 cells were harvested and washed twice with ice-cold phosphate-buffered saline. The cells were then immobilized on slides by cytospin (63) and fixed with 4% paraformaldehyde (in PBS, pH 7.4, 1 h, room temperature). The cells were then washed with PBS and incubated in permeabilization solution (0.1% Triton-X-100 in 0.1% sodium citrate in phosphate-buffered saline, 30 min, room temperature). The permeabilization solution was then removed, TUNEL reaction mixture (50 μL) added, and the cells were incubated (1 h, 37 °C) in a humidified chamber. The cells were washed again with phosphate-buffered saline and counterstained with 1 μg/mL DAPI (4′,6′-diamidino-2-phenylindole) in phosphate-buffered saline for 10 min to identify cellular nuclei. Incidence of apoptosis was assessed under a fluorescence microscope using a FITC filter. Cells with TUNEL-positive nuclei were considered apoptotic. DAPI staining was used to determine the total number of cells in a field. A minimum of six fields per slide were used to calculate the percent of cells that were apoptotic.

DNA laddering—Harvested INS-1 cells were washed three times with phosphate-buffered saline and resuspended in 500 μL of lysis buffer (100 mM Tris-HCl [pH 8.5], 5 mM EDTA, 0.2 M NaCl, 0.2% w/v SDS, and 0.2 mg/mL proteinase K). After a 90 min incubation-period on ice, the lysates were centrifuged (10,000g, 10 min, 4 °C). The DNA in the supernatant was precipitated overnight with an equal volume of 100% (v/v) ethanol at −20 °C. The DNA precipitate was washed once with 70% ethanol and resuspended in 30 μL of 10 mM Tris-HCl mM EDTA (pH 7.5) buffer supplemented with 200 μg/mL DNase-free RNase A. After incubation at 37 °C for 2 h, the DNA was analyzed using 2% agarose gel electrophoresis. DNA laddering, which reflects apoptosis-associated DNA fragmentation, was visualized using ethidium bromide staining under UV light.

Assessment of mitochondrial membrane potential (MitoMP) by flow cytometry —Loss of MitoMP is an important step in the induction of cellular apoptosis (71). INS-1 cell MitoMP was measured using a commercial kit according to the manufacturer's instructions. Briefly, harvested cells were washed once with phosphate-buffered saline and resuspended in 100 μL of the same buffer (~10^5 cells/mL). An aliquot (5 μL) of Mito Flow fluorescent reagent was added and the cell suspension was incubated at 37 °C for 30 min. The cells were then transferred to fluorescence-activated cell sorting tubes and diluted 1:5 with buffer provided in the kit. Fluorescence in cells was analyzed by flow cytometry (BD Biosciences, San Jose, CA) at an excitation wavelength of 488 nm.

Ceramide analyses by electrospray ionization (ESI)/MS/MS

Lipids were extracted from INS-1 cells under acidic conditions, as described (72,73). Briefly, cells were harvested, gently pelleted, and extraction buffer (chloroform/methanol/2% acetic acid, 2/2/1.8; v/v/v) containing C8-ceramide (C8-ceramide, *m/z* 432) internal standard (IS, 500 ng) was added to the cellular pellet. After vigorous vortexing, the mixture was centrifuged (800g) and the organic bottom layer was collected, concentrated to dryness under nitrogen and reconstituted in chloroform/methanol (1/4) containing 10 pmol/μL LiOH. To measure ceramide content, ESI/MS/MS standard curves were generated from a series of samples containing fixed amount of C8-ceramide standard and varied amounts of long-chain ceramide standards. The relative abundances of individual ceramide species, relative to the C8-ceramide internal standard, were measured by ESI/MS/MS scanning for constant neutral loss of 48, which reflects the elimination of formaldehyde and water from the $[M + Li]^+$ ion (63). This loss is characteristic of ceramide-Li^+ adducts upon low energy collisionally-activated

dissociation ESI/MS/MS (72). Lipid phosphorous measurements were used to normalize individual ceramide molecular species.

Sphingomyelin (sphingomyelin) analyses by ESI/MS/MS

Sphingomyelins are formed by reaction of a ceramide with CDP-choline and similar to glycerophosphocholine (GPC) lipids, they contain a phosphocholine as the polar head group. This feature of sphingomyelins facilitates identification of sphingomyelin molecular species by constant neutral loss scanning of trimethylamine ($[M + Li]^+$ -$N(CH_3)_3$) or constant neutral loss of 59, as described (74). The prominent ions in the total ion current spectrum are those of the even mass PC molecular species and these mask the odd mass sphingomyelin signals. Constant neutral loss of 59, however, facilitates emergence of signals for sphingomyelin species at odd *m/z* values, reflecting loss of nitrogen. Lipid extracts prepared as above were used for the sphingomyelin analyses. In the absence of individual sphingomyelin species availability, sphingomyelins content in the samples was determined based on standard curves generated using commercially-available brain and egg sphingomyelins with known percentage of each fatty acid constituent and 14:0/14:0-GPC (*m/z* 684, 8 μg) as internal standard. Lipid phosphorous measurements were used to normalize individual sphingomyelin molecular species.

Quantitative RT-PCR

To determine mRNA expression of key enzymes involved in ceramide-generating pathways, total RNA was isolated from INS-1 cells using RNeasy kit (Qiagen Inc.). cDNA was then synthesized using SuperScriptII kit (Invitrogen) and heat-inactivated (70 °C for 15 min). A reaction without reverse transcriptase was performed to verify the absence of genomic DNA. PCR amplifications were performed using SYBR Green PCR kit (Invitrogen) in an ABI 7000 detection system (Applied Biosystems). The primers were designed based on known rat sequences for neutral sphingomyelinase (NSMase), serine palmitoyl transferase (SPT), ceramidase, and internal control 18S provided in the Gene Bank™ database with accession numbers AB047002, XM001053124, AF214647, and X01117, respectively. The sense/antisense primer sets were as follows: NSMase, ccggatgcacactacttcagaa/ggattgggtgtctggagaaca; SPT, caccgagcactatgggatca/cgagcgcattctccatgtta; ceramidase, tgaaagccaccttcgagattg/ctgagtatgtctgccctgtatgct; and 18S control, agtcctgccctttgtacaca/gatccgagggcctcactaaac.

Generation of NSMase-KD cells using siRNA

Two hairpin-forming oligonucleotides directed against NSMase mRNA were selected using SiRNA design tool (http://bioinfo.clontech.com/rnaidesigner/frontpage.jsp) and cloned into RNAi-Ready pSIREN Retro-Q, according to manufacturer's instructions. The two sequences were gatccGCAGGACTTCCAGTACTTAAAttcaagagatttaagtactggaagtcctgcttttttg and gatccGCACGTCTATACTCTCAATGGttcaagagaccattgagagtatagacgtgcttttttg, where the targeting sequences within the synthetic oligonucleotides are capitalized. Constructs that express the sRNAis were pSIREN-NSMase-1 and pSIREN-NSMase-2. Retroviruses were packaged in PT67 cells and used to infect INS-1 cells. A construct that encoded scrambled RNA was used to generate control cell lines. Cells were selected with 0.25 μg/mL puromycin and single cell clones were expanded. Total RNA was prepared from the various cell lines and Northern blot analyses, as described (75), was performed to identify cell lines in which NSMase mRNA was knocked down. Cell lines of interest were selected for further expansion and study.

Statistical analyses

Data were converted to mean ± standard error of the means and the Students' t-test was applied to determine significant differences between two samples ($p < 0.05$). Statistical differences

between multiple treatment groups and a control group were determined using analysis of variances and Dunnett post-hoc test.

RESULTS

Demonstration of iPLA$_2$β overexpression in INS-1 cells

In the present study, we examined the relationship between iPLA$_2$β, ceramides, and INS-1 cell apoptosis during ER stress. This was done in INS-1 insulinoma cells because they manifest endogenous iPLA$_2$β activity analogous to that expressed in pancreatic islet β-cells, are susceptible to ER stress, provide an abundant source of starting material, and can be manipulated to over or under express proteins of interest (43,54,63). To more directly examine a role of iPLA$_2$β in ER stress-induced INS-1 cell apoptosis, parallel studies were done with iPLA$_2$β-overexpressing INS-1 cells (OE INS-1 cells). These cells, relative to empty-vector transfected INS-1 cells (V INS-1 cells), expressed higher iPLA$_2$β protein in the cytosol (Figure 1A *insert*) and as reported earlier (43), nearly 15-fold higher iPLA$_2$β catalytic activity (V, 79 ± 8 and OE, 1386 ± 434 pmole/mg protein/min, n = 5 in each group). As expected, iPLA$_2$β catalytic activity manifested in the transfected INS-1 cells exhibited characteristic properties of the enzyme; stimulation by ATP (V, 272 ± 18 and OE, 3688 ± 503, pmole/mg protein/min) and inhibition by BEL (residual activity near zero in both groups).

ER stress-induced INS-1 cell apoptosis is amplified in iPLA$_2$β-OE INS-1 cells

In light of the earlier observation of higher incidence of apoptosis of OE INS-1 cells (63), in the present study, we examined if progression of apoptosis due to thapsigargin-induced ER stress differed in V and OE INS-1 cells. Because the incidence of INS-1 cell apoptosis during the first 11 h was unchanged, only data from vehicle-treated and cells treated with thapsigargin for 12 and 24 h are presented. TUNEL staining analyses (Figure 1A) revealed that the abundance of TUNEL-positive INS-1 cells was minimal at 0 h and progressively increased following treatment with thapsigargin for 12 and 24 h in both V and OE INS-1 cells. The abundance of apoptotic cells in the OE group at 24 h, however, was 2-fold greater than in the V group.

As accurate quantitation of TUNEL-positive cells is not easily achieved, incidence of apoptosis following induction of ER-stress in the INS-1 cells with thapsigargin was assessed by two additional methods. In the DNA laddering assay shown in Figure 1B, DNA fragmentation, which occurs in cells undergoing apoptosis, was not detected in the V group at 12 h but was evident at 24 h. In contrast, DNA fragmentation in the OE group was detectable by 12 h and was more pronounced at 24 h than in the V group. The second assay measured loss of MitoMP, which is another hallmark of cellular apoptosis, in a suspension of cells to which a fluorescent Mito Flow reagent is added. This reagent concentrates in the mitochondria of healthy cells but the mitochondria of cells undergoing apoptosis become compromised and accumulate less of the reagent and this is reflected by a decrease in the fluorescence signal and the appearance of a second peak that is left of the original. The spectra presented in Figure 1C reflect fluorescence measurement in 10,000 INS-1 cells and the percentage of cells losing MitoMP, analyzed by the application software, is indicated as M1. As illustrated, there was a gradual appearance of a second peak over a 24 h-period of ER stress, indicative of a rise in the number of INS-1 cells with compromised MitoMP. However, relative to the V group, a second peak begins to emerge in the OE group by 12 h suggesting that the MitoMP is affected in a higher number of cells in this group by this time (V, 22.00 ± 0.01% and OE, 25.04 ± 0.01%, p = 0.004965, n = 5 in each group). At 24 h, a greater percentage of OE INS-1 cells were seen to lose MitoMP, relative to the V INS-1 cells.

Thapsigargin induces expression of GRP78, CHOP, and PAPR in INS-1 cells

To confirm induction of ER stress in INS-1 cells treated with thapsigargin, expression of ER stress factors GRP78 and CHOP was examined in cytosol prepared from vehicle- and thapsigargin-treated INS-1 cells. Immunoblotting analyses revealed induction of both within 2–4 h (Figure 2A). To quantify their expression levels, the density of GRP78 and CHOP immunoreactivity to the internal control tubulin immunoreactivity at corresponding times was determined. Representative analyses illustrated in Figures 2B and 2C indicated increases in GRP78 between 2 and 4 h and in CHOP between 4 and 8 h. They further revealed that between 4 and 16 h, expression of both was greater in the OE group than in the V group. A key protein that is selectively cleaved at the onset of apoptosis by caspases is poly(ADP-ribose) polymerase (PARP) (76). Cleavage of PARP leads to generation of an active product that facilitates cellular disassembly (77). In both V and OE INS-1 cells thapsigargin-induced ER stress resulted in cleavage of PARP (Figure 2D) but it occurred earlier and was more profound in the OE than in the V group. Collectively, the data presented in Figures 1–2 reveal a sequence of thapsigargin-induced events that are characteristic of an ER stress response in INS-1 cells beginning with expression of GRP78 followed by CHOP, cleavage of PARP, and finally apoptotic cell-death.

ER stress induces increases in neutral sphingomyelinase message levels in INS-1 cells and this is inhibited by BEL

We previously reported temporal increases in ceramide generation in INS-1 cells during a 24 h-period following induction of ER stress (63). A rise in cellular ceramide levels can occur via *de novo* synthesis, sphingomyelin breakdown, or decreased degradation of ceramides. To determine which pathway is prominent in INS-1 cells undergoing ER stress, total RNA was prepared from vehicle-treated and thapsigargin-treated INS-1 cells for quantitative PCR analyses of enzymes in each pathway: serine palmitoyl transferase (SPT), which catalyzes the rate limiting step in the *de novo* pathway; neutral sphingomyelinase (NSMase), which catalyzes the hydrolysis of sphingomyelins; and ceramidase, which catalyzes the degradation of ceramides. As shown in Figure 3A, mRNA levels for SPT were not significantly altered while ceramidase message expression decreases over the course of ER stress. In contrast, ER stress increased NSMase mRNA expression in the INS-1 cells and its expression in the OE INS-1 cells was found to be more sensitive to ER stress, as reflected by the earlier onset of increase in these cells, relative to the V INS-1 cells (2 vs. 6 h). Additionally, steady-state levels of NSMase message reached between 12–16 h were 2-fold higher in the OE INS-1 cells than in the V INS-1 cells.

The increased sensitivity of NSMase expression to ER stress and the amplification of the increase in iPLA$_2$β-overexpressing INS-1 cells suggested that NSMase expression might be modulated by iPLA$_2$β. To test this possibility, ER stress was induced in OE INS-1 cells in the absence or presence of BEL. At 12 h following induction of ER stress, the cells were harvested for quantitative PCR analyses. As shown in Figure 3B, BEL not only reduced control levels of NSMase expression but almost completely prevented the induction of NSMase expression at 12 h. In contrast, ceramidase mRNA levels, which were decreased similarly in ER-stressed V and OE INS-1 cells, were not returned to basal levels by BEL. A small decrease in SPT mRNA levels was seen in control V INS-1 cells but there was no significant effect of BEL in the ER-stressed INS-1 cells. These findings suggest that ER stress induces iPLA$_2$β-mediated expression of NSMase in INS-1 cells.

ER stress induces increases in ER-associated iPLA$_2$β protein and catalytic activity and concomitant NSMase protein expression that is inhibited by inactivation of iPLA$_2$β with BEL

To further examine the link between ER stress, iPLA$_2$β activation, and NSMase expression the affects of ER stress on ER-associated iPLA$_2$β were first examined. ER fraction was

prepared from V and OE INS-1 cells using an ER-isolation kit and organelle marker analyses verified that this fraction was enriched in ER protein calnexin, but not in proteins associated with other organelles (data not shown). As shown in Figure 4A, ER stress led to temporal accumulations in ER-associated iPLA$_2$β protein between 2–8 h. This was reflected by increases in ER associated iPLA$_2$β catalytic activity (Fig. 4B). Both iPLA$_2$β protein accumulation and catalytic activity in the ER during ER stress were greater in the OE INS-1 cells, relative to V INS-1 cells.

We next examined whether induction of NSMase message during ER stress leads to increased expression of NSMase protein and whether this could be inhibited by inactivation of iPLA$_2$β. As seen in Figure 4C, a temporal increase in NSMase protein expression is seen in ER stressed INS-1 cells, with the increases being greater in the OE INS-1 cells. Pretreatment of the INS-1 cells with BEL for 1 h prior to induction of ER stress resulted in inhibition of induction of NSMase protein for up to 16 h. During this period, iPLA$_2$β catalytic activity was inhibited in the V INS-1 cells by 95, 78, 83, and 78% and by 97, 90, 79, and 58% in the OE INS-1 cells at 0, 4, 8, 16h, respectively. These findings support and strengthen an association between NSMase expression and iPLA$_2$β activation in ER-stressed INS-1 cells.

ER stress induces decreases in the relative abundances of sphingomyelin molecular species in INS-1 cells

To allow quantitation of INS-1 cell sphingomyelins, standard curves for various molecular species were first constructed. Because commercially-available synthetic sphingomyelins were not available when these studies were initiated, natural sphingomyelins from egg and brain (Avanti Polar Lipids, Alabaster, AL) were used. To identify the individual species, the amounts of the natural sphingomyelins were varied in the presence of a constant amount of an internal standard and ESI/MS/MS with constant neutral loss scanning of 59 ($[M + Li]^+ -N(CH_3)_3$) was performed. 14:0/14:0-glycerophosphocholine (GPC, *m/z* 684) was used as the internal standard because it does not occur naturally in rats, mice, humans, or INS-1 cells. Next, the sphingomyelins were saponified to liberate the individual fatty acids and their ratios determined using d8-arachidonic acid as internal standard. The percent contribution of individual fatty acids to the total fatty acid content of each source was then determined and used to construct standard curves of the individual sphingomyelin species (Figure 5).

To determine whether induction of NSMase mRNA during ER stress is associated with increased sphingomyelin hydrolysis, lipid extracts were prepared in the presence of the 14:0/14:0-GPC internal standard from vehicle-treated and ER-stressed INS-1 cells and analysed by ESI/MS/MS. As shown in Figure 6A (*insert*), the prominent ions in the total ion current spectrum of GPC are those of the even mass PC species. The emergence of the odd *m/z* sphingomyelin species is facilitated by constant neutral loss of 59 (Figure 6A). Figure 6 displays the positive ion ESI-MS TIC tracing of Li^+ adducts of the sphingomyelin species in INS-1 cell lipids after addition of the 14:0/14:0-GPC internal standard, which is represented in the spectrum by its $[M + Li]^+$ ion (*m/z* 684). As with the ceramide species, the major sphingomyelin species endogenous to INS-1 cells are 16:0 (*m/z* 709), 18:0 (*m/z* 737), 22:0 (*m/z* 793), 24:1 (*m/z* 819), and 24:0 (*m/z* 821). The spectra were acquired by monitoring constant neutral loss of 59 in V and OE INS-1 cells treated with either vehicle (Figures 6A and C) or thapsigargin (Figures 6B and D). Following induction of ER stress, the relative abundances of the sphingomyelins in both V (Figure 6B) and OE (Figure 6D) INS-1 cells decreased, as reflected by the decreases in the intensities of ions representing them.

ER stress-induced generation of ceramides and sphingomyelin hydrolysis in INS-1 cells are inhibited by BEL

To examine whether iPLA$_2$β participates in ceramide generation or sphingomyelin hydrolysis in ER stressed INS-1cells, the cells were treated with thapsigargin in the absence or presence of BEL, a suicide inhibitor of iPLA$_2$β. In the absence of ER stress, the total ceramide pool in INS-1 cells was found to be similar (V, 8.37 ± 2.01 and OE, 8.18 ± 2.17 nmol/μmol PO_4). ER stress induced an increase in all of the identified ceramide species in both V and OE INS-1 cells (Table 1) and the increase in total ceramide pool was two-fold higher in the OE than in the V INS-1 cells (Figure 7A). BEL alone had no effect in the absence of ER stress (data were therefore combined with corresponding control groups) but addition of BEL to ER-stressed cells resulted in inhibition of ceramide generation.

In the absence of ER stress, the total sphingomyelin pools in the V and OE INS-1 cells were also not found to be different (V, 118 ± 14 and OE, 111± 12 pmol/μmol PO_4). Quantitation of individual sphingomyelin species revealed decreases in the major endogenous sphingomyelin species in both V and OE INS-1 cells subjected to ER stress, reflecting an increase in sphingomyelin hydrolysis (Table 2). And as shown in Figure 7B, ER stress induced a two-fold greater decrease in the total sphingomyelin pool in the OE group, in comparison with the V group. Addition of BEL resulted in prevention of ER stress-induced decreases in sphingomyelin hydrolysis in both V and OE INS-1 cells. The data presented in Tables 1 and 2 and Figures 3–6 therefore suggest that ER stress induces NSMase expression in INS-1 cells leading to hydrolysis of sphingomyelins and generation of ceramides, and that iPLA$_2$β participates in this process.

ER stress-induced ceramide generation, sphingomyelin hydrolysis, and INS-1 cell apoptosis are suppressed by inhibition of NSMase but not the de novo synthesis pathway

We next examined whether sphingomyelin hydrolysis or the *de novo* synthesis pathway is the more important contributor to the generation of ceramides in ER-stressed INS-1 cells. Lipids were extracted from INS-1 cells treated with either vehicle or thapsigargin in the absence or presence of either the SPT inhibitor *l*-cycloserine (LCS) or the NSMase inhibitor GW4869 (GW). These inhibitors and the concentrations of the inhibitors used in the present study have been widely used to distinguish ceramide-generating pathways in various cell systems, including pancreatic islets (78,79). ESI/MS/MS analyses used to determine the ceramide and sphingomyelin contents revealed a lack of effect of inhibitor treatment alone (data were therefore combined with corresponding controls). LCS also failed to prevent ER stress-induced changes in ceramides or sphingomyelins (Tables 1 and 2; Figures 8A and 8B). In contrast, GW4869 suppressed both the increase in ceramide generation and decrease in sphingomyelins in the ER-stressed INS-1 cells. These data taken together with the finding of increased NSMase, but not SPT, message expression suggest that ER stress-induced ceramide generation in INS-1 cells most likely occurs via increased hydrolysis of sphingomyelins.

As *de novo* synthesis of ceramides was reported to participate in lipoapoptosis of β-cells (79), the possibility that this pathway may also contribute to ER stress-induced INS-1cell apoptosis was examined. As reflected by DNA laddering and MitoMP analyses (Figures 8C and 8D, respectively), treatment with the inhibitor alone had no effect and LCS was unable to prevent ER stress-induced INS-1 cell apoptosis. In contrast, inhibition of NSMase prevented DNA fragmentation and significantly suppressed compromising of MitoMP in ER-stressed INS-1 cells. Collectively, these findings suggest that NSMase-mediated increases in ceramide generation, but not *de novo* synthesis of ceramides, contribute to ER stress-mediated INS-1 cell apoptosis.

Knock-down (KD) of NSMase suppresses ER stress-induced ceramide generation, sphingomyelin hydrolysis, and INS-1 cell apoptosis

To further establish the relationship between ER stress, iPLA$_2$β, NSMase, and INS-1cell apoptosis, we used sRNAi technology to generate INS-1 cells in which NSMase is knocked-down (KD). This protocol resulted in the identification by Northern analyses of V and OE INS-1 cell lines in which NSMase was knocked down. One OE cell line (OE KD3) in which sRNAi treatment failed to suppress NSMase message was included as a negative control. As illustrated in Figure 9A, NSMase-KD completely prevented induction of NSMase message in ER-stressed INS-1 cells. As expected, induction of NSMase was not suppressed in the OE-KD3 cells.

We next determined whether knock-down of NSMase is able to suppress ER stress-induced affects on ceramides, sphingomyelins, and INS-1cell apoptosis. Quantitation of ceramides and sphingomyelins in untreated (c)ontrol (V and OE INS-1 cells infected with construct encoded with scrambled RNA) and NSMase-KD V and OE INS-1 cells were found to be similar and pooled separately and presented as “V C” and “OE C” bars. As the data in thapsigargin-treated V KD and OE KD1 and KD2 INS-1 cells were similar, they were pooled and presented as a single “KDT” bar. Similarly, as the data obtained in thapsigargin-treated OE KD3 cells were similar to thapsigargin-treated OE INS-1 cells, they were pooled and presented as a single “ OE T” bar. As illustrated in Figure 9, NSMase-KD completely abolished ER stress-induced increases in ceramide generation (Figure 9B) and sphingomyelin hydrolysis (Figure 9C) in ER-stressed INS-1cells. DNA laddering analyses (Figure 9D) revealed that ER stress induced with thapsigargin promoted DNA fragmentation in the V, OE, and OE KD3 INS-1 cells, but not in the VKD or OEKD INS-1 cells. The findings further support an involvement of NSMase in ER stress-induced INS-1cell apoptosis.

DISCUSSION

It is becoming widely accepted that apoptosis plays a prominent role in the loss of β-cells during the progression of diabetes mellitus (2,10,11,14,16–20,80–82). It is therefore important to gain a better understanding of the processes that lead to apoptotic β-cell death, so that more targeted therapeutic measures can be used to prevent or delay this process. Among the recognized apoptotic signaling pathways (22,23), β□-cell death in the Akita diabetic (15,21) and NOD.k iHEL nonimmune (83) diabetic mouse models have been reported to be due to ER stress. Wolfram syndrome, which is associated with juvenile-onset diabetes mellitus, is also thought to be a consequence of chronic ER stress in pancreatic β-cells (80–82). These reports raise the possibility that the ER stress pathway contributes to β-cell losses in diabetes. However, very little is currently known about the cellular events that are triggered by ER stress and that eventually lead to β-cell apoptosis. As such, elucidation of the mechanisms that contribute to ER stress-induced β-cell apoptosis is very much warranted.

Earlier findings in insulinoma cells (39) and pancreatic islets (40) using inhibitors of SERCA to deplete ER Ca^{2+} stores (38) suggested that the Group VIA Ca^{2+}-independent PLA$_2$ (iPLA$_2$β) participates in ER stress-induced β-cell apoptosis. We have since demonstrated that ER stress induces apoptosis of INS-1 insulinoma cells and that the incidence of apoptosis (a) is inhibited by BEL, a suicide-inhibitor of iPLA$_2$β, (b) is amplified in OE INS-1 cells, and (c) correlates with the expression levels of iPLA$_2$β protein and activity (63). These findings are consistent with a role for iPLA$_2$β in ER stress-induced β-cell apoptosis.

A puzzling finding in that study was that ER stress also induced ceramide generation in INS-1. Further, the ceramides reached higher levels in iPLA$_2$β-overexpressing INS-1 cells, suggesting that iPLA$_2$β might mediate ceramide generation in INS-1 cells during ER stress. Accumulations in cellular levels of ceramides can be achieved by an increase in *de novo*

synthesis from palmitate and other precursors (79) or hydrolysis of sphingomyelins resulting in the generation of ceramide and phosphocholine (84), or by a decrease in degradation of ceramide (85,86). The *de novo* pathway is thought to participate in lipoapoptosis of β-cells (79,86), but, as yet, there are no studies which examined ceramide generation during ER stress. In view of our earlier findings, it was therefore of interest to determine (a) which ceramide-generating pathway contributes to ceramide generation in ER-stressed INS-1 cells, (b) if $iPLA_2\beta$ is a requisite, and (c) whether inhibition of this pathway prevents ER stress-induced INS-1cell apoptosis.

Similar to the earlier study (63), thapsigargin triggered an ER stress response (15,35,36), induced apoptosis, and increased ceramide accumulation in INS-1 cells in the present study. To examine whether INS-1 cell accumulations in ceramides during ER stress require $iPLA_2\beta$, ER stress was induced in INS-1 cells in the absence or presence of BEL and lipids were extracted for ESI/MS/MS analyses of ceramides (73). Such analyses revealed five major ceramide species that are endogenous to the INS-1 cells and nearly all of the ceramide species were increased in ER-stressed INS-1 cells. Inhibition of $iPLA_2\beta$ with BEL, however, completely prevented the increase in the total ceramide pool. These findings were taken to indicate that $iPLA_2\beta$ contributes to the rise in ceramides in INS-1 cells during ER stress.

As ceramide formation can be increased by different pathways, quantitative PCR analyses were used to examine message levels of ceramide-generating enzymes to determine the source of the ceramide increases in INS-1 cells during ER stress. They included serine palmitoyl transferase (SPT), which catalyzes the rate-limiting step in *de novo* synthesis of ceramides (79); neutral sphingomyelinase (NSMase), which hydrolyzes sphingomyelins to generate ceramides and phosphocholine (84); and the ceramide-degrading enzyme ceramidase, inactivation of which by nitric oxide could lead to ceramide accumulations (85).

Unexpectedly, ER stress did not induce SPT message expression but increased NSMase mRNA and protein levels in the INS-1 cells. This is in contrast to earlier reports that *de novo* synthesis of ceramides contributes to lipoapoptosis of β-cells in ZDF rats (79) and of pancreatic islets exposed to free fatty acids (86,87). The increases in NSMase levels seen in our studies were accompanied by increases in sphingomyelin hydrolysis, as reflected by decreases in sphingomyelin molecular species, identified by ESI/MS/MS analyses (74). Analogous to the effects of BEL on ceramide increases, both the increases in NSMase message and protein expression and sphingomyelin hydrolysis in ER-stressed INS-1 cells were inhibited by BEL. Further, chemical inhibition of NSMase activity or knock-down of NSMase were not only effective in preventing ceramide generation and sphingomyelin hydrolysis in ER-stressed INS-1 cells but they also suppressed ER stress-induced INS-1 cell apoptosis. In contrast, inhibition of the *de novo* pathway was ineffective in preventing these consequences of ER stress in INS-1 cells. The ER stress pathway and the consequences of its induction that included increases in ceramide generation, NSMase, sphingomyelin hydrolysis, and apoptosis were all accelerated and/or amplified in $iPLA_2\beta$-overexpressing (OE) INS-1 cells. As in the V INS-1 cells, inhibition of $iPLA_2\beta$ or NSMase were effective in preventing these ER stress-induced effects in the OE INS-1 cells, but inhibition of the *de novo* pathway was not. An alternate salvage pathway where sphingoid bases generated by hydrolysis of complex sphingolipids by ceramidase are recycled into ceramides has recently been reported to also increase ceramide formation (88). While this pathway was not examined directly in the present study, the findings that ER stress did not increase mRNA levels of either ceramidase or of iNOS (data not presented) might be taken to mean that the salvage pathway is most likely not a major pathway during ER stress in INS-1 cells. In fact, mRNA levels for ceramidase were modestly decreased by ER stress and they remained unaffected by inhibition of $iPLA_2\beta$ with BEL. Our data therefore suggest that ceramides generated via hydrolysis of sphingomyelins by NSMase

contributes to ER stress-induced INS-1 cell apoptosis and strongly support a role for iPLA$_2$β in activating this pathway.

While further studies are needed to elucidate the process by which ER stress affects iPLA$_2$β and iPLA$_2$β induces NSMase expression, a potential mechanism might be gleaned by considering the present findings along with our earlier observations (63). In that study, ER stress was shown to stimulate iPLA$_2$β activity and its perinuclear localization in INS-1 cells. As membranes of the nucleus and ER are contiguous (89,90), perinuclear accumulation of iPLA$_2$β is consistent with association of the iPLA$_2$β protein with a subcellular compartment that is likely to include ER (89). That this in fact is occurring is supported by the present observation of increases in ER-associated iPLA$_2$β protein and catalytic activity in the ER stressed INS-1 cells. The ER in β-cells is enriched in arachidonate-containing phospholipids (91) and the increases in iPLA$_2$β protein would amplify the hydrolysis and subsequent metabolism of arachidonic acid. It is not unlikely that arachidonic acid and/or its bioactive metabolites (eicosanoids) stimulate the activity of NSMase in β-cells, as they do in other cell types (92–96), especially since there is evidence for NSMase in both nuclei and ER (97,98). Alternatively, arachidonic acid or eicosanoids, by virtue of their ability to regulate transcription of several gene families (99), could induce NSMase expression. This possibility is supported by the present findings that inactivation of iPLA$_2$β by BEL also inhibits NSMase message and protein expression and that NSMase-KD INS-1 cells are resistant to ER stress-induced ceramide accumulation and apoptosis. These findings taken together with earlier demonstrations of inhibition of AA hydrolysis and eicosanoids generation in β-cells and INS-1 cells by BEL (54,55,61,62,91,100), strengthen the possibility that ER stress activates iPLA$_2$β, leading to the induction of NSmase and increased generation of ceramides via this pathway. The various proposed roles of ceramides in cellular processes only raises the complexity of the potential mechanism(s) by which they could promote β-cell death during ER stress. It remains to be determined whether one molecular species of ceramide is more active and essential than another or whether a rise in ceramides or a decrease in sphingomyelins (101) is a more important factor in promoting β-cell death.

In summary, our findings demonstrate for the first time a link between ER stress-induced INS-1 insulinoma cell apoptosis, NSMase-mediated generation of ceramides, and iPLA$_2$β activation. Our observations therefore raise the importance of gaining a better understanding of the role of iPLA$_2$β, not only in ER stress-mediated effects, but also its potential role in β-cell apoptosis, a process that is gaining recognition as a major contributor to β-cell losses during the progression of diabetes.

References

1. Tisch R, McDevitt H. Insulin-dependent diabetes mellitus. Cell 1996;85:291–297. [PubMed: 8616883]
2. Mathis D, Vence L, Benoist C. Beta-cell death during progression to diabetes. Nature 2001;414:792–798. [PubMed: 11742411]
3. DeFronzo RA. Lilly lecture 1987. The triumvirate: beta-cell, muscle, liver. A collusion responsible for NIDDM. Diabetes 1988;37:667–687. [PubMed: 3289989]
4. DeFronzo RA. Insulin resistance: a multifaceted syndrome responsible for NIDDM, obesity, hypertension, dyslipidaemia and atherosclerosis. Neth J Med 1997;50:191–197. [PubMed: 9175399]
5. Kahn CR. Diabetes. Causes of insulin resistance. Nature 1995;373:384–385. [PubMed: 7830788]
6. Kudva, YC.; Butler, PC. Insulin secretion in type 2 diabetes mellitus. In: Draznin, B.; Rizza, R., editors. Clinicl Research in Diabetes and Obesity. Humana Press; Totowa, N.J.: 1997. p. 119-136.
7. Clark A, Wells CA, Buley ID, Cruickshank JK, Vanhegan RI, Matthews DR, Cooper GJ, Holman RR, Turner RC. Islet amyloid, increased A-cells, reduced B-cells and exocrine fibrosis: quantitative changes in the pancreas in type 2 diabetes. Diabetes Res 1988;9:151–159. [PubMed: 3073901]

8. Kloppel G, Lohr M, Habich K, Oberholzer M, Heitz PU. Islet pathology and the pathogenesis of type 1 and type 2 diabetes mellitus revisited. Surv Synth Pathol Res 1985;4:110–125. [PubMed: 3901180]
9. Stefan Y, Orci L, Malaisse-Lagae F, Perrelet A, Patel Y, Unger RH. Quantitation of endocrine cell content in the pancreas of nondiabetic and diabetic humans. Diabetes 1982;31:694–700. [PubMed: 6131002]
10. Butler AE, Janson J, Bonner-Weir S, Ritzel R, Rizza RA, Butler PC. β-Cell deficit and increased β-cell apoptosis in humans with type 2 diabetes. Diabetes 2003;52:102–110. [PubMed: 12502499]
11. Yoon KH, Ko SH, Cho JH, Lee JM, Ahn YB, Song KH, Yoo SJ, Kang MI, Cha BY, Lee KW, Son HY, Kang SK, Kim HS, Lee IK, Bonner-Weir S. Selective β-cell loss and α-cell expansion in patients with type 2 diabetes mellitus in Korea. J Clin Endocrinol Metab 2003;88:2300–2308. [PubMed: 12727989]
12. Bernard C, Berthault M-F, Saulnier C, Ktorza A. Neogenesis vs. apoptosis as main components of pancreatic β-cell mass changes in glucose-infused normal and mildly diabetic adult rats. FASEB J 1999;13:1195–1205. [PubMed: 10385610]
13. Vinik A, Rafaeloff R, Pittenger G, Rosenberg L, Duguid W. Induction of pancreatic islet neogenesis. Horm Metab Res 1997;29:278–293. [PubMed: 9230349]
14. Butler AE, Janson J, Soeller WC, Butler PC. Increased β-cell apoptosis prevents adaptive increase in β-cell mass in mouse model of type 2 diabetes: evidence for role of islet amyloid formation rather than direct action of am. Diabetes 2003;52:2304–2314. [PubMed: 12941770]
15. Oyadomari S, Koizumi A, Takeda K, Gotoh T, Akira S, Araki E, Mori M. Targeted disruption of the CHOP gene delays endoplasmic reticulum stress-mediated diabetes. J Clin Invest 2002;109:525–532. [PubMed: 11854325]
16. Pick A, Clark J, Kubstrup C, Levisetti M, Pugh W, Bonner-Weir S, Polonsky KS. Role of apoptosis in failure of beta-cell mass compensation for insulin resistance and beta-cell defects in the male Zucker diabetic fatty rat. Diabetes 1998;47:358–364. [PubMed: 9519740]
17. Cerasi E, Kaiser N, Leibowitz G. Type 2 diabetes and beta cell apoptosis. Diabetes Metab 2000;26:13–16. [PubMed: 10945145]
18. Chandra J, Zhivotovsky B, Zaitsev S, Juntti-Berggren L, Berggren P, Orrenius S. Role of apoptosis in pancreatic beta-cell death in diabetes. Diabetes 2001;50:S44–47. [PubMed: 11272200]
19. Mandrup-Poulsen T. Beta-cell apoptosis: stimuli and signaling. Diabetes 2001;50:S58–63. [PubMed: 11272204]
20. Sesti G. Apoptosis in the beta cells: cause or consequence of insulin secretion defect in diabetes? Ann Med 2002;34:444–450. [PubMed: 12523500]
21. Oyadomari S, Araki E, Mori M. Endoplasmic reticulum stress-mediated apoptosis in pancreatic beta-cells. Apoptosis 2002;7:335–345. [PubMed: 12101393]
22. Diaz-Horta O, Kamagate A, Herchuelz A, Van Eylen F. Na/Ca exchanger overexpression induces endoplasmic reticulum-related apoptosis and caspase-12 activation in insulin-releasing BRIN-BD11 cells. Diabetes 2002;51:1815–1824. [PubMed: 12031969]
23. Mehmet H. Caspases find a new place to hide. Nature 2000;403:29–30. [PubMed: 10638735]
24. Bitko V, Barik S. An endoplasmic reticulum-specific stress-activated caspase (caspase-12) is implicated in the apoptosis of A549 epithelial cells by respiratory syncytial virus. J Cell Biochem 2001;80:441–454. [PubMed: 11135374]
25. Nakagawa T, Zhu H, Morishima N, Li E, Xu J, Yankner B, Yuan J. Caspase-12 mediates endoplasmic-reticulum-specific apoptosis and cytotoxicity by amyloid-beta. Nature 2000;403:98–103. [PubMed: 10638761]
26. Rao RV, Castro-Obregon S, Frankowski H, Schuler M, Stoka V, del Rio G, Bredesen DE, Ellerby HM. Coupling endoplasmic reticulum stress to the cell death program. AN Apaf-1-independent intrinsic pathway. J Biol Chem 2002;277:21836–21842. [PubMed: 11919205]
27. Aridor M, Balch WE. Integration of endoplasmic reticulum signaling in health and disease. Nat Med 1999;5:745–751. [PubMed: 10395318]
28. Ron D. Translational control in the endoplasmic reticulum stress response. J Clin Invest 2002;110:1383–1388. [PubMed: 12438433]
29. Harding HP, Ron D. Endoplasmic Reticulum Stress and the Development of Diabetes: A Review. Diabetes 2002;51:S455–461. [PubMed: 12475790]

30. Cohen GM. Caspases: the executioners of apoptosis. Biochem J 1997;326:1–16. [PubMed: 9337844]
31. Kaufman RJ. Stress signaling from the lumen of the endoplasmic reticulum: coordination of gene transcriptional and translational controls. Genes Dev 1999;13:1211–1233. [PubMed: 10346810]
32. Harding HP, Zeng H, Zhang Y, Jungries R, Chung P, Plesken H, Sabatini DD, Ron D. Diabetes mellitus and exocrine pancreatic dysfunction in $PERK^{-/-}$ mice reveals a role for translational control in secretory cell survival. Cell Press 2001;7:1153–1163.
33. Delepine M, Nicolino M, Barrett T, Golamaully M, Lathrop GM, Julier C. EIF2AK3, encoding translation initiation factor 2-alpha kinase 3, is mutated in patients with Wolcott-Rallison syndrome. Nat Genet 2000;25:406. [PubMed: 10932183]
34. Takeda K, Inoue H, Tanizawa Y, Matsuzaki Y, Oba J, Watanabe Y, Shinoda K, Oka Y. WFS1 (Wolfram syndrome 1) gene product: predominant subcellular localization to endoplasmic reticulum in cultured cells and neuronal expression in rat brain. Hum Mol Genet 2001;10:477–484. [PubMed: 11181571]
35. Araki E, Oyadomari S, Mori M. Impact of endoplasmic reticulum stress pathway on pancreatic β-cells and diabetes mellitus. Experimental Biology and Medicine 2003;228:1213–1217. [PubMed: 14610263]
36. Zinszner H, Kuroda M, Wang X, Batchvarova N, Lightfoot RT, Remotti H, Stevens JL, Ron D. CHOP is implicated in programmed cell death in response to impaired function of the endoplasmic†reticulum. Genes Dev 1998;12:982–995. [PubMed: 9531536]
37. Araki E, Oyadomari S, Mori M. Endoplasmic reticulum stress and diabetes mellitus. Intern Med 2003;42:7–14. [PubMed: 12583611]
38. Thastrup O, Dawson AP, Scharff O, Foder B, Cullen PJ, Drobak BK, Bjerrum PJ, Christensen SB, Hanley MR. Thapsigargin, a novel molecular probe for studying intracellular calcium release and storage. 1989. Agents Actions 1994;43:187–193. [PubMed: 7725971]
39. Zhou Y-P, Teng D, Dralyuk F, Ostrega D, Roe MW, Philipson L, Polonsky KS. Apoptosis in insulin-secreting cells. Evidence for the role of intracellular Ca^{2+} stores and arachidonic acid metabolism. J Clin Invest 1998;101:1623–1632. [PubMed: 9541492]
40. Nowatzke W, Ramanadham S, Ma Z, Hsu FF, Bohrer A, Turk J. Mass spectrometric evidence that agents that cause loss of Ca^{2+} from intracellular compartments induce hydrolysis of arachidonic acid from pancreatic islet membrane phospholipids by a mechanism that does not require a rise in cytosolic Ca^{2+} concentration. Endocrinology 1998;139:4073–85. [PubMed: 9751485]
41. Gijon MA, Leslie CC. Phospholipases A_2. Semin Cell Dev Biol 1997;8:297–303. [PubMed: 10024493]
42. Schaloske RH, Dennis EA. The phospholipase A_2 superfamily and its group numbering system. Biochimica et Biophysica Acta (BBA) - Molecular and Cell Biology of Lipids In Press. Corrected Proof
43. Ma Z, Ramanadham S, Wohltmann M, Bohrer A, Hsu FF, Turk J. Studies of insulin secretory responses and of arachidonic acid incorporation into phospholipids of stably transfected insulinoma cells that overexpress group VIA phospholipase A_2 ($iPLA_2\beta$) indicate a signaling rather than a housekeeping role for $iPLA_2\beta$. J Biol Chem 2001;276:13198–208. [PubMed: 11278673]
44. Mancuso DJ, Jenkins CM, Gross RW. The genomic organization, complete mRNA sequence, cloning, and expression of a novel human intracellular membrane-associated calcium-independent phospholipase A_2. J Biol Chem 2000;275:9937–9945. [PubMed: 10744668]
45. Tanaka H, Takeya R, Sumimoto H. A novel intracellular membrane-bound calcium-independent phospholipase A_2. Biochem Biophys Res Commun 2000;272:320–326. [PubMed: 10833412]
46. Ma Z, Ramanadham S, Kempe K, Chi XS, Ladenson J, Turk J. Pancreatic islets express a Ca^{2+}-independent phospholipase A_2 enzyme that contains a repeated structural motif homologous to the integral membrane protein binding domain of ankyrin. J Biol Chem 1997;272:11118–27. [PubMed: 9111008]
47. Balsinde J, Bianco ID, Ackermann EJ, Conde-Frieboes K, Dennis EA. Inhibition of calcium-independent phospholipase A_2 prevents arachidonic acid incorporation and phospholipid remodeling in P388D1 macrophages. PNAS 1995;92:8527–8531. [PubMed: 7667324]
48. Boilard E, Surette ME. Anti-CD3 and concanavalin A-induced human t cell proliferation is associated with an increased rate of arachidonate-phospholipid remodeling. Lack of involvement of group iv

and group VI phospholipase A_2 in remodeling and increased susceptibility of proliferating T cells to CoA-independent transacylase inhibitor-induced apoptosis. J Biol Chem 2001;276:17568–17575. [PubMed: 11278296]

49. Isenovic E, LaPointe MC. Role of Ca^{2+}-Independent Phospholipase A_2 in the Regulation of Inducible Nitric Oxide Synthase in Cardiac Myocytes. Hypertension 2000;35:249–254. [PubMed: 10642306]
50. Maggi LB Jr, Moran JM, Scarim AL, Ford DA, Yoon J-W, McHowat J, Buller RML, Corbett JA. Novel role for calcium-independent phospholipase A_2 in the macrophage antiviral response of inducible nitric-oxide synthase expression. J Biol Chem 2002;277:38449–38455. [PubMed: 12167650]
51. Tithof PK, Olivero J, Ruehle K, Ganey PE. Activation of neutrophil calcium-dependent and -independent phospholipases A_2 by organochlorine compounds. Toxicol Sci 2000;53:40–47. [PubMed: 10653519]
52. Williams SD, Ford DA. Calcium-independent phospholipase A_2 mediates CREB phosphorylation and c-fos expression during ischemia. Am J Physiol Heart Circ Physiol 2001;281:H168–176. [PubMed: 11406482]
53. Moran JM, Buller RML, McHowat J, Turk J, Wohltmann M, Gross RW, Corbett JA. Genetic and pharmacologic evidence that calcium-independent phospholipase $A_2\beta$ regulates virus-induced inducible nitric-oxide synthase expression by macrophages. J Biol Chem 2005;280:28162–28168. [PubMed: 15946940]
54. Ramanadham S, Hsu F-F, Bohrer A, Ma Z, Turk J. Studies of the role of group vi phospholipase A_2 in fatty acid incorporation, phospholipid remodeling, lysophosphatidyl-choline generation, and secretagogue-induced arachidonic acid release in pancreatic islets and insulinoma cells. J Biol Chem 1999;274:13915–13927. [PubMed: 10318801]
55. Ramanadham S, Song H, Hsu FF, Zhang S, Crankshaw M, Grant GA, Newgard CB, Bao S, Ma Z, Turk J. Pancreatic islets and insulinoma cells express a novel isoform of group VIA phospholipase A_2 (iPLA$_2\beta$) that participates in glucose-stimulated insulin secretion and is not produced by alternate splicing of the iPLA$_2\beta$ transcript. Biochemistry 2003;42:13929–40. [PubMed: 14636061]
56. Atsumi, G-i; Tajima, M.; Hadano, A.; Nakatani, Y.; Murakami, M.; Kudo, I. Fas-induced arachidonic acid release is mediated by Ca^{2+}-independent phospholipase A_2 but not cytosolic phospholipase A_2, which undergoes proteolytic inactivation. J Biol Chem 1998;273:13870–13877. [PubMed: 9593733]
57. Atsumi, G-i; Murakami, M.; Kojima, K.; Hadano, A.; Tajima, M.; Kudo, I. Distinct roles of two intracellular phospholipase A_2s in fatty acid release in the cell death pathway. Proteolytic fragment of type IVA cytosolic phospholipase $A_2\alpha$ inhibits stimulus-induced arachidonate release, whereas that of type VI Ca^{2+}-independent phospholipase A_2 augments spontaneous fatty acid release. J Biol Chem 2000;275:18248–18258. [PubMed: 10747887]
58. Wilson HA, Allred DV, O'Neill K, Bell JD. Activities and interactions among phospholipases A_2 during thapsigargin-induced S49 cell death. Apoptosis 2000;5:389–396. [PubMed: 11227220]
59. Shin KJ, Chung C, Hwang YA, Kim SH, Han MS, Ryu SH, Suh P. Phospholipase A_2-mediated Ca^{2+} influx by 2,2′,4,6-tetrachlorobiphenyl in PC12 cells. Toxicol Appl Pharmacol 2002;78:37–43. [PubMed: 11781078]
60. Tithof PK, Elgayyar M, Cho Y, Guan WEI, Fisher AB, Peters-Golden M. Polycyclic aromatic hydrocarbons present in cigarette smoke cause endothelial cell apoptosis by a phospholipase A_2-dependent mechanism. FASEB J 2002;16:1463–1464. [PubMed: 12205049]
61. Gross RW, Ramanadham S, Kruszka KK, Han X, Turk J. Rat and human pancreatic islet cells contain a calcium ion independent phospholipase A_2 activity selective for hydrolysis of arachidonate which is stimulated by adenosine triphosphate and is specifically localized to islet beta-cells. Biochemistry 1993;32:327–36. [PubMed: 8418853]
62. Ramanadham S, Gross RW, Han X, Turk J. Inhibition of arachidonate release by secretagogue-stimulated pancreatic islets suppresses both insulin secretion and the rise in beta-cell cytosolic calcium ion concentration. Biochemistry 1993;32:337–46. [PubMed: 8418854]
63. Ramanadham S, Hsu FF, Zhang S, Jin C, Bohrer A, Song H, Bao S, Ma Z, Turk J. Apoptosis of insulin-secreting cells induced by endoplasmic reticulum stress is amplified by overexpression of group VIA calcium-independent phospholipase A_2 (iPLA$_2\beta$) and suppressed by inhibition of iPLA$_2\beta$. Biochemistry 2004;43:918–930. [PubMed: 14744135]

64. Jayadev S, Liu B, Bielawska AE, Lee JY, Nazaire F, Pushkareva MY, Obeid LM, Hannun YA. Role for ceramide in cell cycle arrest. J Biol Chem 1995;270:2047–2052. [PubMed: 7836432]

65. Obeid LM, Hannun YA. Ceramide: a stress signal and mediator of growth suppression and apoptosis. J Cell Biochem 1995;58:191198.

66. Venable ME, Lee JY, Smyth MJ, Bielawska A, Obeid LM. Role of ceramide in cellular senescence. J Biol Chem 1995;270:30701–30708. [PubMed: 8530509]

67. Coffin, JM.; Hart, GW. Retrovirus. Cold Spring Harbor, Laboratory Press; Cold Spring Harbor, New York: 1996.

68. Ma Z, Zhang S, Turk J, Ramanadham S. Stimulation of insulin secretion and associated nuclear accumulation of iPLA$_2$β in INS-1 insulinoma cells. Am J Physiol Endocrinol Metab 2002;282:E820–33. [PubMed: 11882502]

69. Dallner G. Isolation of rough and smooth microsomes--general. Methods Enzymol 1974;31(Pt A): 191–201. [PubMed: 4418022]

70. Depierre, JW.; Dallner, G. Isolation, subfractionation, and characterization of the endoplasmic reticulum. 3. John Wiley; New York, NY: 1976.

71. Desagher S, Osen-Sand A, Nichols A, Eskes R, Montessuit S, Lauper S, Maundrell K, Antonsson B, Martinou J-C. Bid-induced conformational change of Bax is responsible for mitochondrial cytochrome c release during apoptosis. J Cell Biol 1999;144:891–901. [PubMed: 10085289]

72. Hsu FF, Turk J. Characterization of ceramides by low energy collisional-activated dissociation tandem mass spectrometry with negative-ion electrospray ionization. J Am Soc Mass Spectrom 2002;13:558–570. [PubMed: 12019979]

73. Hsu FF, Turk J, Stewart ME, Downing DT. Structural studies on ceramides as lithiated adducts by low energy collisional-activated dissociation tandem mass spectrometry with electrospray ionization. J Am Soc Mass Spectrom 2002;13:680–695. [PubMed: 12056568]

74. Hsu FF, Turk J. Structural determination of sphingomyelin by tandem mass spectrometry with electrospray ionization. J Am Soc Mass Spectrom 2000;11:437–449. [PubMed: 10790848]

75. Bao S, Miller DJ, Ma Z, Wohltmann M, Eng G, Ramanadham S, Moley K, Turk J. Male mice that do not express group via phospholipase A_2 produce spermatozoa with impaired motility and have greatly reduced fertility. J Biol Chem 2004;279:38194–38200. [PubMed: 15252026]

76. Nicholson DW, Thornberry NA. Caspases: killer proteases. Trends in Biochemical Sciences 1997;22:299–306. [PubMed: 9270303]

77. Oliver FJ, de la Rubia G, Rolli V, Ruiz-Ruiz MC, de Murcia G, Murcia JM-d. Importance of Poly (ADP-ribose) polymerase and its cleavage in apoptosis. lesson from an uncleavable mutant. J Biol Chem 1998;273:33533–33539. [PubMed: 9837934]

78. Marchesini N, Luberto C, Hannun YA. Biochemical properties of mammalian neutral sphingomyelinase2 and its role in sphingolipid metabolism. J Biol Chem 2003;278:13775–13783. [PubMed: 12566438]

79. Shimabukuro M, Higa M, Zhou Y-T, Wang M-Y, Newgard CB, Unger RH. Lipoapoptosis in beta-cells of obese prediabetic fa/fa rats. Role of serine palmitoyltransferase overexpression. J Biol Chem 1998;273:32487–32490. [PubMed: 9829981]

80. Fonseca SG, Fukuma M, Lipson KL, Nguyen LX, Allen JR, Oka Y, Urano F. WFS1 is a novel component of the unfolded protein response and maintains homeostasis of the endoplasmic reticulum in pancreatic β-cells. J Biol Chem 2005;280:39609–39615. [PubMed: 16195229]

81. Ueda K, Kawano J, Takeda K, Yujiri T, Tanabe K, Anno T, Akiyama M, Nozaki J, Yoshinaga T, Koizumi A, Shinoda K, Oka Y, Tanizawa Y. Endoplasmic reticulum stress induces WFS1 gene expression in pancreatic β-cells via transcriptional activation. Eur J Endocrinol 2005;153:167–176. [PubMed: 15994758]

82. Yamada T, Ishihara H, Tamura A, Takahashi R, Yamaguchi S, Takei D, Tokita A, Satake C, Tashiro F, Katagiri H, Aburatani H, Miyazaki J-i, Oka Y. WFS1-deficiency increases endoplasmic reticulum stress, impairs cell cycle progression and triggers the apoptotic pathway specifically in pancreatic β-cells. Hum Mol Genet 2006;15:1600–1609. [PubMed: 16571599]

83. Socha L, Silva D, Lesage S, Goodnow C, Petrovsky N. The role of endoplasmic reticulum stress in nonimmune diabetes: NOD.k iHEL, a novel model of β-cell death. Ann NY Acad Sci 2003;1005:178–183. [PubMed: 14679055]

84. Hannun YA. The sphingomyelin cycle and the second messenger function of ceramide. J Biol Chem 1994;269:3125–3128. [PubMed: 8106344]
85. Franzen R, Fabbro D, Aschrafi A, Pfeilschifter J, Huwiler A. Nitric oxide induces degradation of the neutral ceramidase in rat renal mesangial cells and is counterregulated by protein kinase. J Biol Chem 2002;277:46184–46190. [PubMed: 12359735]
86. Kelpe CL, Moore PC, Parazzoli SD, Wicksteed B, Rhodes CJ, Poitout V. Palmitate inhibition of insulin gene expression is mediated at the transcriptional level via ceramide synthesis. J Biol Chem 2003;278:30015–30021. [PubMed: 12771145]
87. Lupi R, Dotta F, Marselli L, Del Guerra S, Masini M, Santangelo C, Patane G, Boggi U, Piro S, Anello M, Bergamini E, Mosca F, Di Mario U, Del Prato S, Marchetti P. Prolonged exposure to free fatty acids has cytostatic and pro-apoptotic effects on human pancreatic islets: evidence that β-cell death is caspase mediated, partially dependent on ceramide pathway, and Bcl-2 regulated. Diabetes 2002;51:1437–1442. [PubMed: 11978640]
88. Becker KP, Kitatani K, Idkowiak-Baldys J, Bielawski J, Hannun YA. Selective inhibition of juxtanuclear translocation of protein kinase c βII by a negative feedback mechanism involving ceramide formed from the salvage pathway. J Biol Chem 2005;280:2606–2612. [PubMed: 15546881]
89. Holz GG, Leech CA, Heller RS, Castonguay M, Habener JF. cAMP-dependent mobilization of intracellular Ca^{2+} stores by activation of ryanodine receptors in pancreatic beta-cells. A Ca^{2+} signaling system stimulated by the insulinotropic hormone glucagon-like peptide-1-(7-37). J Biol Chem 1999;274:14147–14156. [PubMed: 10318832]
90. Schievella AR, Regier MK, Smith WL, Lin L-L. Calcium-mediated translocation of cytosolic phospholipase A_2 to the nuclear envelope and endoplasmic reticulum. J Biol Chem 1995;270:30749–30754. [PubMed: 8530515]
91. Ramanadham S, Bohrer A, Gross RW, Turk J. Mass spectrometric characterization of arachidonate-containing plasmalogens in human pancreatic islets and in rat islet beta-cells and subcellular membranes. Biochemistry 1993;32:13499–13509. [PubMed: 8257685]
92. Johns DG, Webb RC. TNF-alpha -induced endothelium-independent vasodilation: a role for phospholipase A_2-dependent ceramide signaling. Am J Physiol Heart Circ Physiol 1998;275:H1592–1598.
93. Robinson BS, Hii CS, Poulos A, Ferrante A. Activation of neutral sphingomyelinase in human neutrophils by polyunsaturated fatty acids. Immunology 1997;91:274–280. [PubMed: 9227328]
94. Taketo MM, Sonoshita M. Phospolipase A_2 and apoptosis. Biochimica et Biophysica Acta (BBA) - Molecular and Cell Biology of Lipids 2002;1585:72–76.
95. Zager RA, Conrad DS, Burkhart K. Ceramide accumulation during oxidant renal tubular injury: mechanisms and potential consequences. J Am Soc Nephrol 1998;9:1670–1680. [PubMed: 9727376]
96. Marchesini N, Hannun YA. Acid and neutral sphingomyelinases: roles and mechanisms of regulation. Biochem Cell Biol 2004;82:27–44. [PubMed: 15052326]
97. Fensome AC, Josephs M, Katan M, Rodrigues-Lima F. Biochemical identification of a neutral sphingomyelinase 1 (NSM1)-like enzyme as the major NSM activity in the DT40 B-cell line: absence of a role in the apoptotic response to endoplasmic reticulum stress. Biochem J 2002;365:69–77. [PubMed: 12071841]
98. Tamiya-Koizumi K, Umekawa H, Yoshida S, Kojima K. Existence of Mg^{2+}-dependent, neutral sphingomyelinase in nuclei of rat ascites hepatoma cells. J Biochem (Tokyo) 1989;106:593–598. [PubMed: 2558112]
99. Jurivich DA, Sistonen L, Sarge KD, Morimoto RI. Arachidonate is a potent modulator of human heat shock gene transcription. PNAS 1994;91:2280–2284. [PubMed: 8134388]
100. Ramanadham S, Wolf MJ, Jett PA, Gross RW, Turk J. Characterization of an ATP-stimulatable Ca^{2+}-independent phospholipase A_2 from clonal insulin-secreting HIT cells and rat pancreatic islets: a possible molecular component of the beta-cell fuel sensor. Biochemistry 1994;33:7442–7452. [PubMed: 8003509]
101. Tepper AD, Ruurs P, Wiedmer T, Sims PJ, Borst J, van Blitterswijk WJ. Sphingomyelin hydrolysis to ceramide during the execution phase of apoptosis results from phospholipid scrambling and alters cell-surface morphology. J Cell Biol 2000;150:155–164. [PubMed: 10893264]

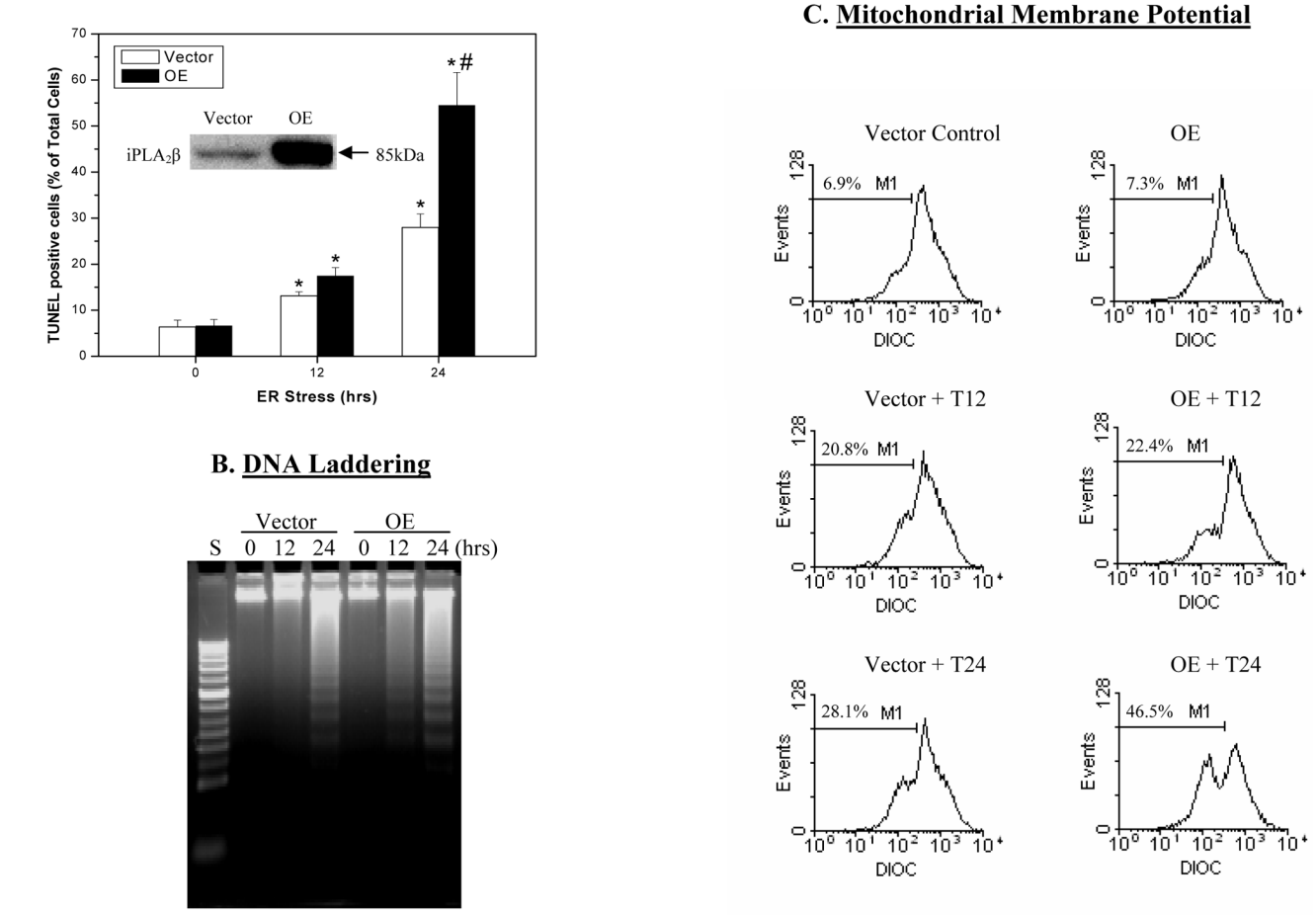

Figure 1. ER stress-induced apoptosis in INS-1 cells

INS-1 cells were treated with either vehicle (DMSO) or with thapsigargin (T, 1 μM) and incubated at 37 °C under an atmosphere of 95%CO_2/5% O_2 for up to 24 h. The cells were collected at 0, 12, and 24 h to determine the incidence of apoptosis. A. TUNEL-positive cells. Percentage of TUNEL-positive cells relative to total number of cells (DAPI-stained) were determined in a minimum of six fields on each slide from each experiment. Data represent mean ± SEM of values obtained from 5–7 separate experiments. (*insert*, iPLA$_2$β-immunoreactive protein). (* Treated groups significantly different from corresponding 0 h control groups, $p < 0.05$. $^{\#}$OE treated group at 24 h significantly different from all other groups, $p < 0.05$.). B. DNA laddering. C. Mitochondrial membrane potential (MitoMP). Representative fluorescence spectra generated from analyses of 10,000 INS-1 cells from each experiment by flow cytometry are presented. M1 refers to the percentage of cells in which MitoMP is compromised. (Each assay was done 3–5 times.)

*We thank the expert technical assistance of Mr. Wu Jin, Dr. Mary Wohltmann, and Ms. Min Tan.

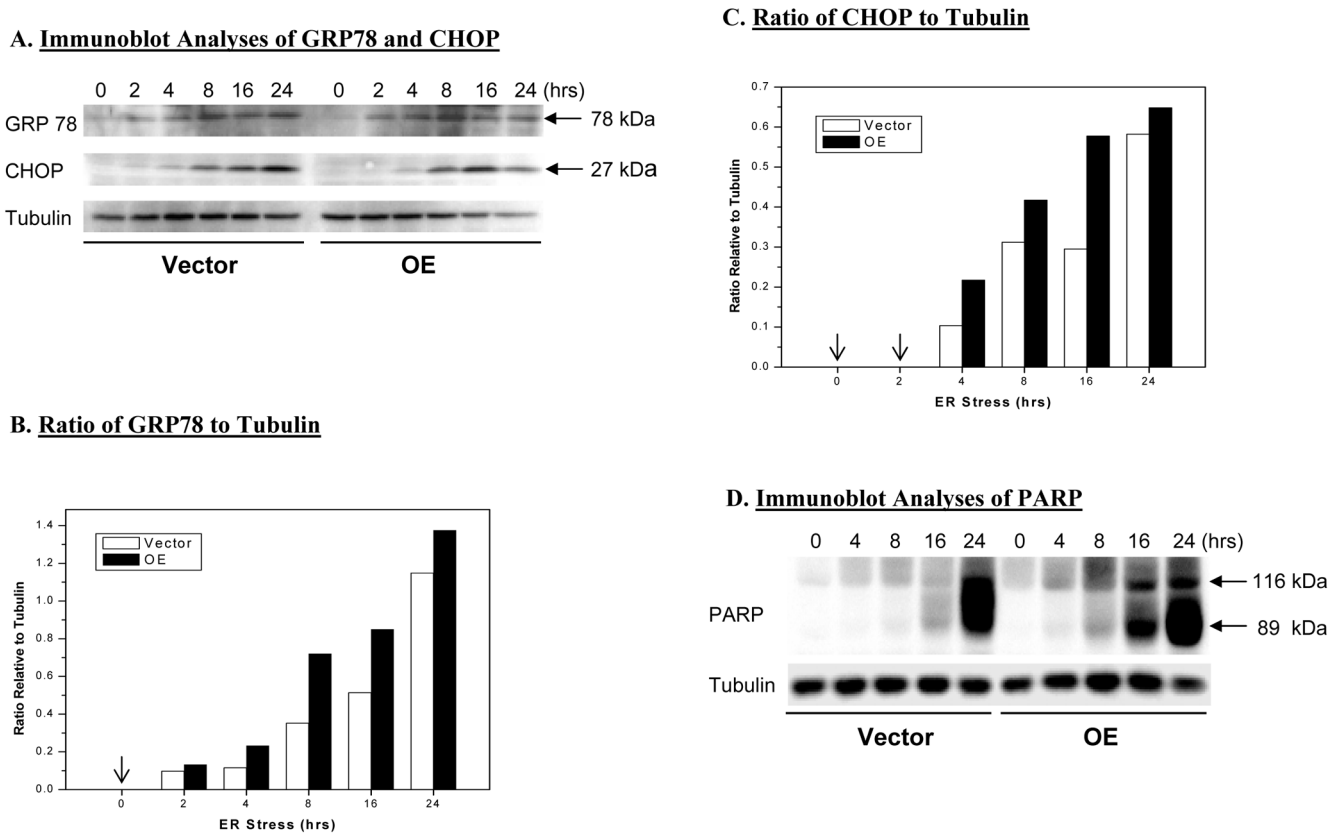

Figure 2. ER stress-induced expression of GRP78, CHOP, and PARP in INS-1 cells

INS-1 cells were treated with either vehicle (DMSO) or with thapsigargin (T, 1 μM). At various times, the cells were harvested and cytosolic fractions prepared and processed for immunoblot analyses. A. ER stress factors GRP78 and CHOP. B and C. Densitometric analyses of GRP78 and CHOP expression, respectively, relative to internal control tubulin. (Arrows indicate non-detectable levels of expression). D. PARP. Immunoreactive bands were visualized by enhanced chemiluminescence. (Each assay was done a minimum of 3 times.)

A. Expression of Messages for Enzymes of Ceramide-Generating Pathways in ER-Stressed INS-1 Cells

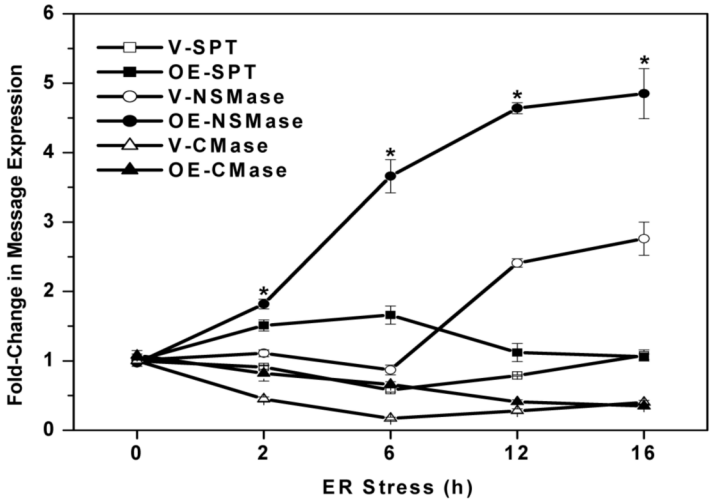

B. Effects of BEL on NSMase, SPT, and CMase Message Expression in ER-Stressed INS-1 Cells

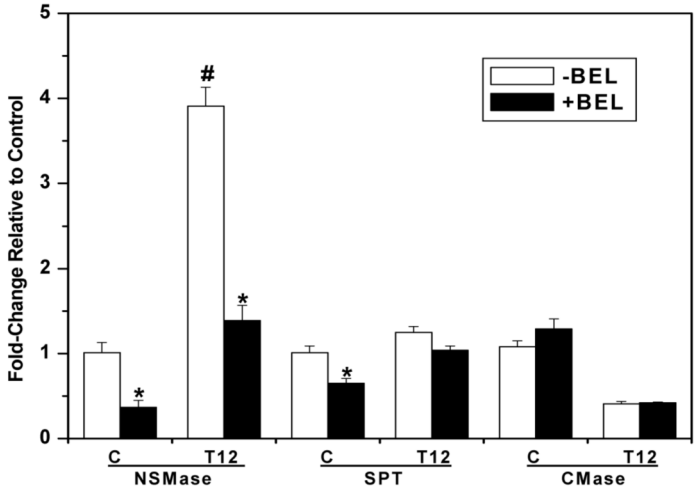

Figure 3. ER stress induced expression of neutral sphingomyelinase (NSMase) message in INS-1 cells ± BEL

INS-1 cells were treated with either vehicle (DMSO, C) or with thapsigargin (T, 1 μM) and cultured for up to 16 h in the absence or presence of BEL (1 μM). Total RNA was prepared from the cells at various times for quantitative (Q) RT-PCR analyses for enzymes that participate in the generation of ceramides via the *de novo* pathway (SPT, serine palmitoyl transferase), sphingomyelin hydrolysis (NSMase), and inhibition of ceramide degradation (CMase, ceramidase). A. QRT-PCR analyses of SPT, NSMase, and CMase (n = 4). (*OE-NSMase group significantly different from V-NSMase group, $p < 0.05$). B. QRT-PCR analyses of NSMase, SPT, and ceramidase ± BEL in control cells and 12 h after induction of ER stress

(T12) (n=4). (*BEL-treated group significantly different from corresponding untreated group, $p < 0.05$. #Untreated NSMase group at 12 h significantly different from other NSMase groups, $p < 0.05$.).

A. ER Stress-Induced Accumulation of iPLA$_2$β Protein in the ER

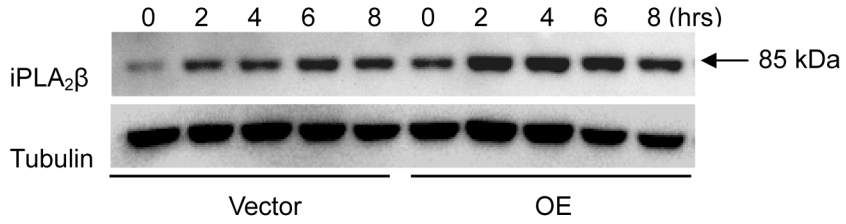

B. ER Stress-Induced Accumulation of iPLA$_2$β Catalytic Activity in the ER

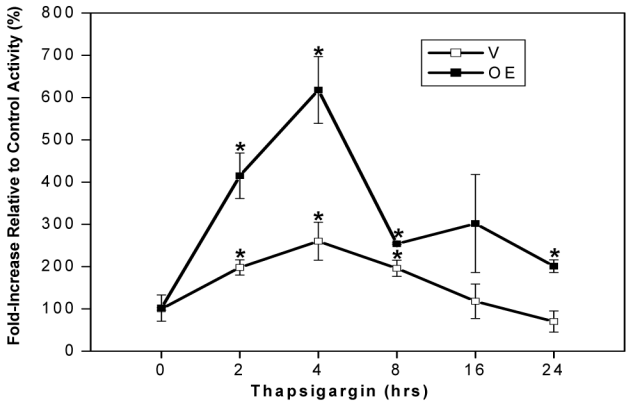

C. ER Stress Induces NSMase Protein Expression in INS-1 Cells and this is Inhibited by BEL

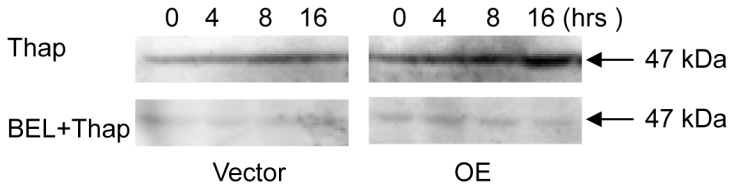

Figure 4. Effects of ER stress on ER-associated iPLA$_2$β and on NSMase protein ± BEL in INS-1 cells

ER fractions were prepared from control and thapsigargin-treated V and OE INS-1 cells to determine ER-associated (A) iPLA$_2$β protein expression and (B) catalytic activity (*Activity significantly different from corresponding untreated basal controls, $p < 0.05$, n= 5–9). C. INS-1 cells were treated without or with BEL (10 μM) for 1 h prior to vehicle or thapsigargin (1 μM) exposure and NSMase protein expression in homogenates was examined by immunoblotting analyses.

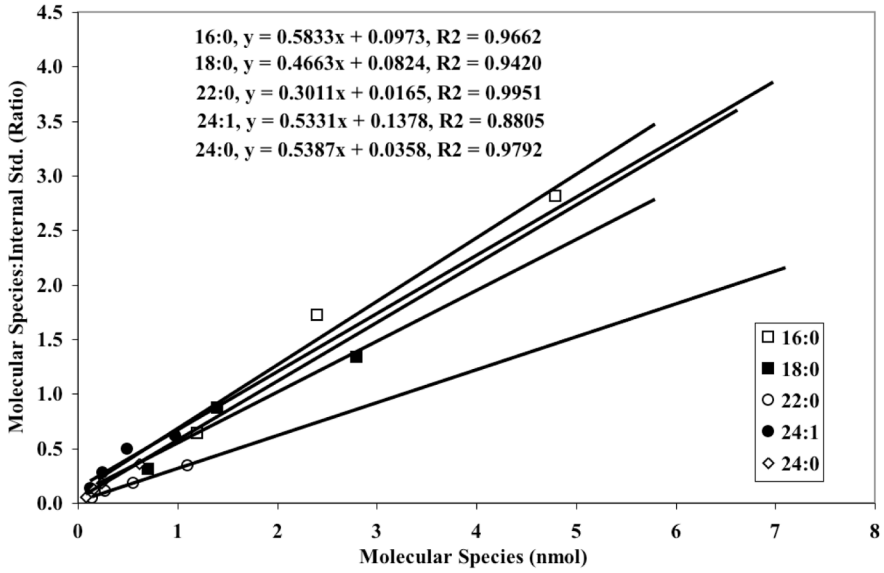

Figure 5. Standard curves for sphingomyelin molecular species

Commercially-available synthetic sphingomyelins from egg and brain were used to construct standard curves in the presence of (14:0/14:0)-GPC internal standard (IS, *m/z* 684), as described in Results. The internal standard concentration was kept constant while varying the concentration of the sphingomyelins.

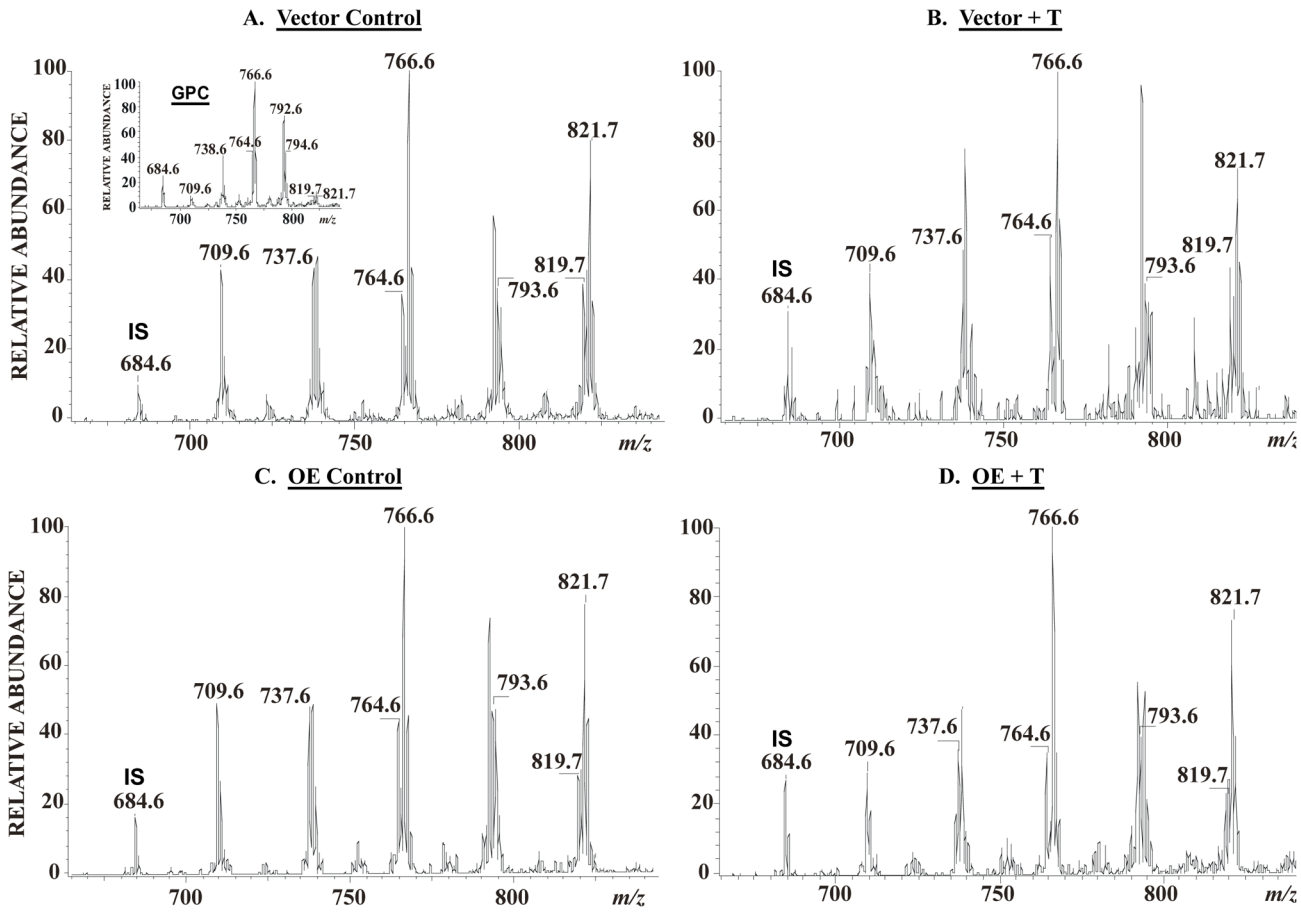

Figure 6. INS-1 cell sphingomyelin analyses by electrospray (ESI) ionization mass spectrometry

INS-1 cells were treated with either vehicle (DMSO, control) or with thapsigargin (T, 1 μM) for 24 h. The cells were detached, washed in phosphate-buffered saline, extraction buffer containing (14:0/14:0)-glycerophosphocholine (GPC) internal standard (IS, *m/z* 684) added to the cells, and lipids extracted under acidic conditions. Relative abundances of sphingomyelin (SM) molecular species were analysed by ESI/MS/MS by monitoring constant neutral loss scanning of 59. A. Vector control. (*insert*, total ion current of GPC). B. Vector + T. C. OE control. D. OE + T. The major sphingomyelin molecular species are indicated in each spectrum: 16:0 (*m/z* 709), 18:0 (*m/z* 737), 22:0 (*m/z* 793). 24:1 (*m/z* 819), and 24:0 (*m/z* 821).

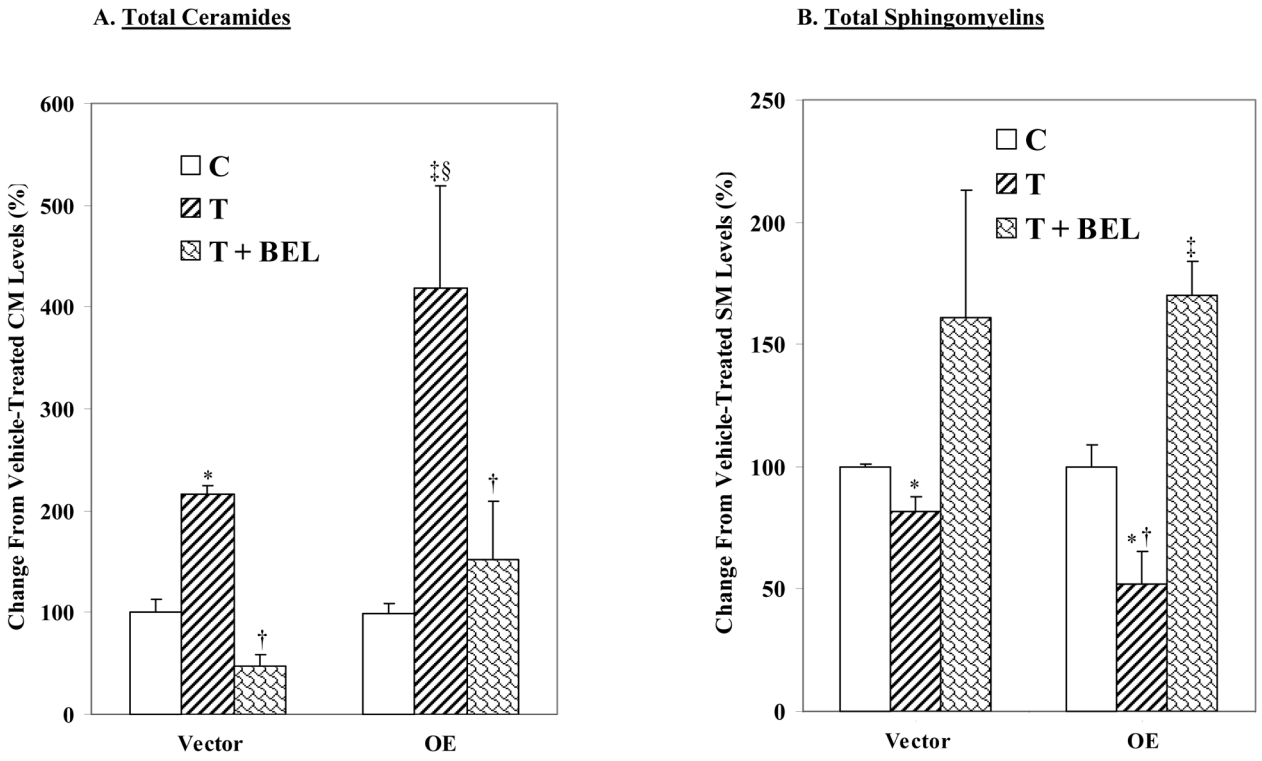

Figure 7. ER stress-induced ceramide generation and sphingomyelin hydrolysis in INS-1 cells are inhibited by BEL

Following MS analyses, the ratios of each ceramide and sphingomyelinmolecular species, relative to internal standard, were determined. The individual molecular species (16:0, 18:0, 22:0. 24:1, and 24:0) were then normalized to total lipid phosphorous content and the change in total ceramide and sphingomyelinpools, relative to ceramide and sphingomyelin pools in untreated control cells, are presented as mean ± SEM (n = 7–9). BEL treatment alone had no significant effect and the data was combined with those from corresponding vehicle-treated groups. A. Total ceramides. (*[and‡]Treated groups significantly different from corresponding control groups at $p < 0.005$ and 0.0005, respectively. [†]BEL-treated groups, significantly different from corresponding treated groups, $p < 0.05$. [§]OET group significantly different from VT group, $p < 0.05$.). B. Total sphingomyelins. (*Treated groups significantly different from corresponding control groups at $p < 0.01$. [†]OET group significantly different from VT, $p < 0.05$. [‡]BEL-treated groups, significantly different from corresponding control and treated groups, $p < 0.05$.)

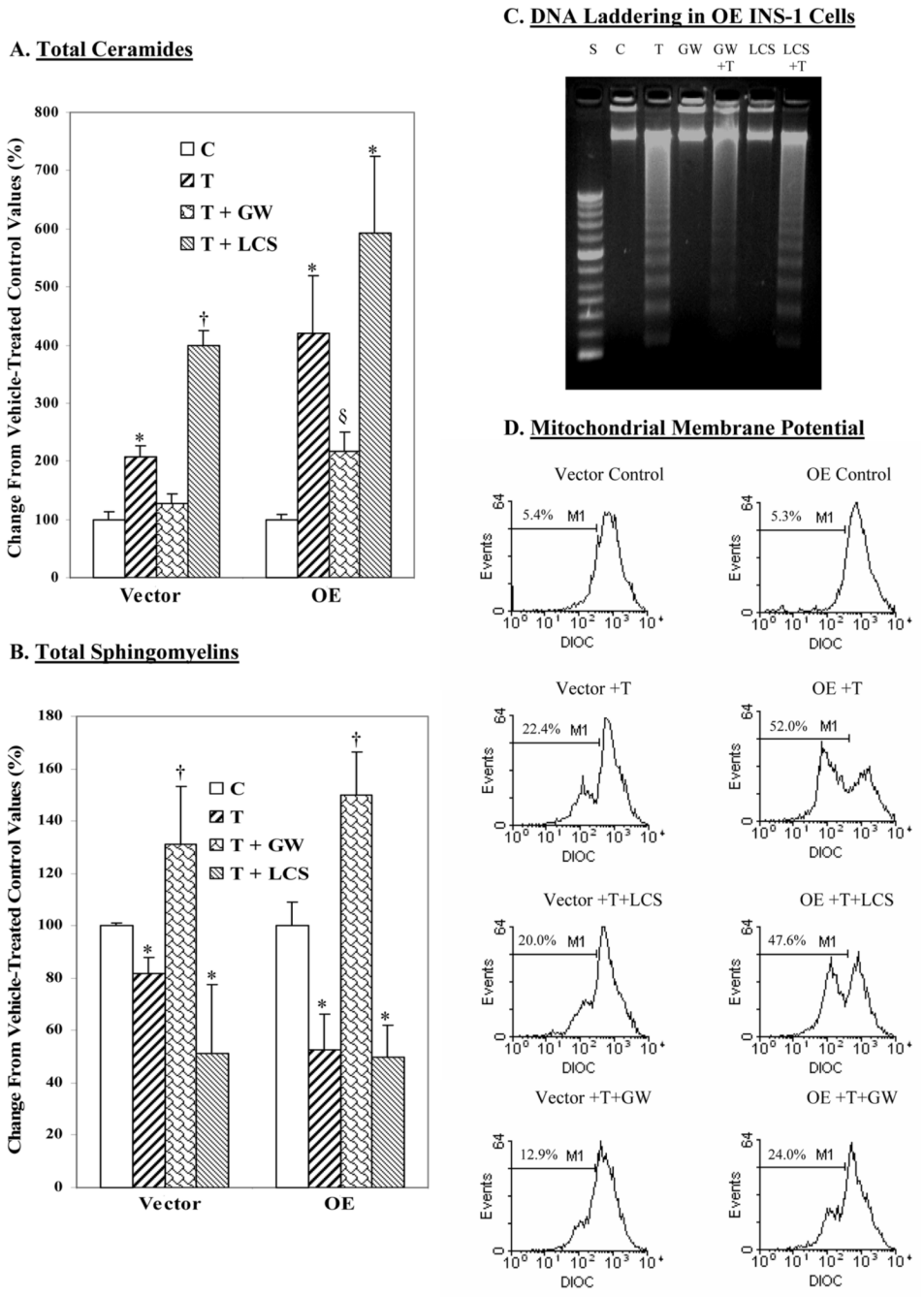

Figure 8. Effects of NSMase and SPT inhibition on ER stress-induced ceramide generation, sphingomyelin hydrolysis, and INS-1 cell apoptosis

INS-1 cells were treated with either vehicle (Control) or with thapsigargin (T, 1 μM) and cultured for up to 24 h in the absence or presence of the NSMase inhibitor GW4869 (GW, 10 μM) or the SPT inhibitor *l*-cycloserine (LCS, 1 mM). At various times, cells were detached and processed for, ceramide, sphingomyelin, and apoptosis analyses. The relative abundances of individual ceramide and sphingomyelin molecular species were analyzed by ESI/MS/MS and quantitated relative to lipid phosphorous. The data are presented as means ± SEM (n = 3–4 in each group) of change in total ceramides and sphingomyelins, relative to untreated control groups. A. Total ceramides. (*Treated groups significantly different from corresponding

control (C) groups, $p < 0.005$. †VT + LCS group significantly different from other vector groups, $p < 0.0001$, §OET + GW significantly different from other OE groups, $p < 0.05$.). B. Total sphingomyelins. (*Significantly different from corresponding control (C) groups, $p < 0.05$. †T + GW groups significantly different from corresponding control (C) groups, $p < 0.01$.). C. DNA laddering. D. MitoMP.

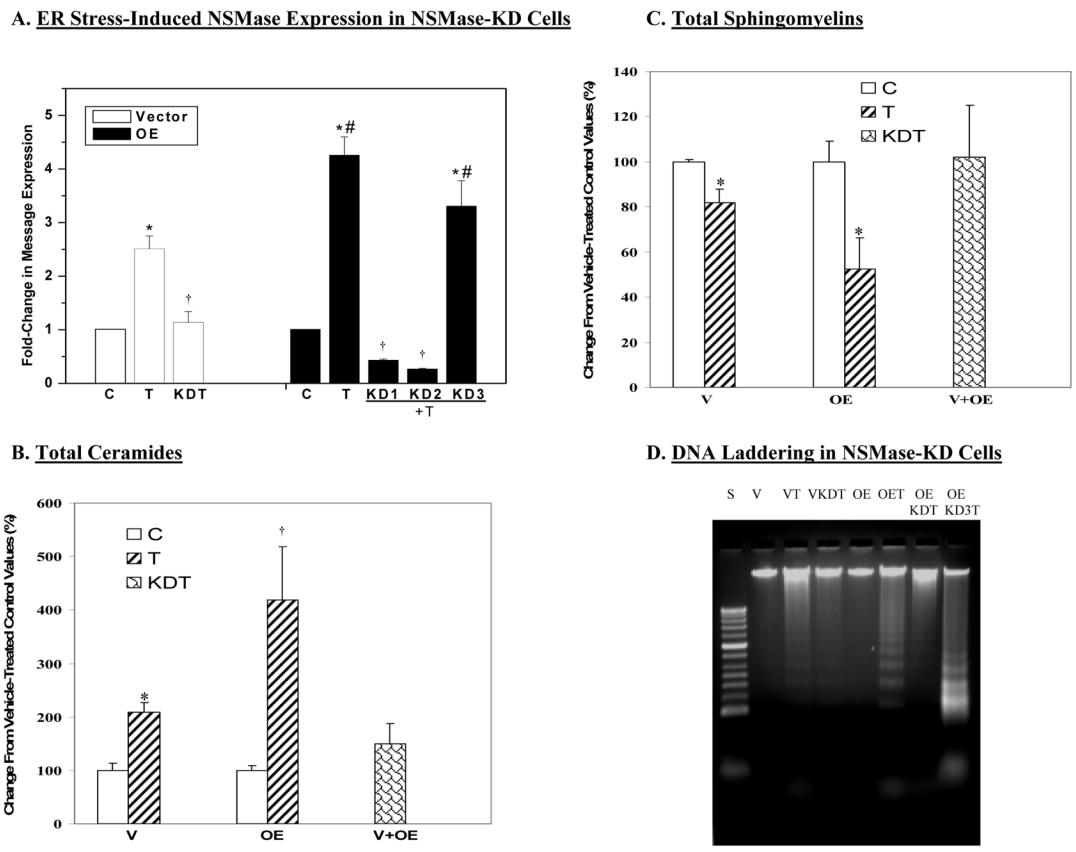

Figure 9. Effects of NSMase knock-down on ER stress-induced ceramide generation, sphingomyelin hydrolysis, and INS-1 cell apoptosis

sRNAi was used to knock-down NSMase in the INS-1 cells. Single cell clones were then cultured to confluency and total RNA was isolated to determine the expression of NSMase message. Selected cell lines were then chosen for further study. A. Effects of ER stress on NSMase expression in NSMase-KD INS-1 cells. Parental INS-1 cells and INS-1 cells in which NSMase was knocked down were treated with either vehicle (DMSO, C) or with thapsigargin (T, 1 μM). The cells were harvested at 16 h and total RNA was prepared for QRT-PCR. The data is expressed as mean fold-change ± SEM, relative to control (n= 4–6). (*Treated groups significantly different from corresponding control groups, $p < 0.05$. †KDT groups significantly different from treated groups, $p < 0.05$. #OE treated groups significantly different from other OE groups, $p < 0.05$.) The relative abundances of individual ceramide and sphingomyelin molecular species were analyzed by ESI/MS/MS and quantitated relative to lipid phosphorous. The data are presented as mean ± SEM (n = 3–4 in each group) of change in total ceramides and sphingomyelins, relative to untreated control groups. As similar results were obtained in vehicle-treated V and V–KD INS-1 cells and OE and OE-KD INS-1 cells, they were pooled into two separate control values and presented as V C and OE C bars, respectively. The measurements in thapsigargin-treated V-KD and OE-KD were also found to be similar and therefore a combined value is presented as a single KDT bar. B. Total ceramides. (*VT group significantly different from corresponding control group, $P < 0.0005$. †OET significantly different from all groups, $p < 0.005$.). C. Total sphingomyelins. (*Treated groups significantly different from corresponding control (C) groups, $p < 0.01$.). D. DNA laddering.

Table 1

Thapsigargin-induced changes in ceramide molecular species in vector (V) and iPLA$_2$β overexpressing (OE) INS-1 cells in the absence and presence of inhibitors

Lipids were extracted from V and OE INS-1 cells and ceramides were analysed by ESI/MS/MS and quantitated. Thapsigargin-induced changes in individual ceramide molecular species in the absence and presence of inhibitors of iPLA$_2$β (BEL, 10 μM), SPT (LCS, 1 μM), or NSMase (GW, 10 μM), relative to corresponding controls, are presented as mean ± SEM.

m/z	C:DB	VC	VT	V+BEL	V+GW	V+LCS	OEC	OET	OE+BEL	OE+GW	OE+LCS
544	**16:0**	100 ± 11	196 ± 27	35 ± 10	157 ± 28	458 ± 74	100 ± 8	340 ± 57	116 ± 46	258 ± 37	560 ± 78
572	**18:0**	100 ± 13	194 ± 24	48 ± 9	146 ± 21	335 ± 138	96 ± 12	379 ± 92	140 ± 65	248 ± 28	742 ± 203
628	**22:0**	100 ± 20	280 ± 106	58 ± 5	99 ± 16	771 ± 0	98 ± 13	670 ± 268	228 ± 47	310 ± 106	1423 ± 363
654	**24:1**	100 ±13	168 ± 20	53 ± 12	114 ± 20	402 ± 54	99 ± 8	401 ± 119	166 ± 48	299 ± 89	741 ± 7
656	**24:0**	100 ± 12	200 ± 24	53 ± 9	121 ± 16	405 ± 88	102 ± 6	305 ± 67	146 ± 77	195 ± 29	542 ± 150

Table 2

Thapsigargin-induced changes in sphingomyelin molecular species in vector (V) and iPLA$_2$β overexpressing (OE) INS-1 cells in the absence and presence of inhibitors

Lipids were extracted from V and OE INS-1 cells and sphingomyelins were analysed by ESI/MS/MS and quantitated. Thapsigargin-induced changes in individual sphingomyelin molecular species in the absence and presence of inhibitors of iPLA$_2$β (BEL, 10 μM), SPT (LCS, 1 μM), or NSMase (GW, 10 μM), relative to corresponding controls, are presented as mean ± SEM.

m/z	C:DB	VC	VT	V+BEL	V+GW	V+LCS	OEC	OET	OE+BEL	OE+GW	OE+LCS
709	**16:0**	100 ± 5	81 ± 9	163 ± 58	129 ± 38	43 ± 21	100 ± 11	59 ± 18	227 ± 49	145 ± 11	34 ± 14
737	**18:0**	100 ± 5	86 ± 11	180 ± 68	109 ± 12	35 ± 30	100 ± 10	52 ± 18	166 ± 20	119 ± 9	31 ± 2
793	**22:0**	100 ± 3	78 ± 12	147 ± 63	147 ± 27	41 ± 35	100 ± 10	45 ± 12	158 ± 10	174 ± 39	31 ± 17
819	**24:1**	100 ± 3	75 ± 7	160 ± 39	130 ± 26	76 ± 13	100 ± 15	55 ± 16	187 ± 18	161 ± 28	125 ± 20
821	**24:0**	100 ± 4	88 ± 13	161 ± 57	130 ± 26	81 ± 17	100 ± 5	75 ± 19	179 ± 5	192 ± 18	103 ±11